

# Advanced Pyrrolidine-Carbamate Self-Immolative Spacer with Tertiary Amine Handle Induces Superfast Cyclative Drug Release

Alberto Dal Corso,<sup>\*[a]</sup> Margaux Frigoli,<sup>[a]</sup> Martina Prevosti,<sup>[a]</sup> Mattia Mason,<sup>[a]</sup> Raffaella Bucci,<sup>[b]</sup> Laura Belvisi,<sup>[a]</sup> Luca Pignataro,<sup>[a]</sup> and Cesare Gennari<sup>\*[a]</sup>

Amine-carbamate self-immolative (SI) spacers represent practical and versatile tools in targeted prodrugs, but their slow degradation mechanism limits drug activation at the site of disease. We engineered a pyrrolidine-carbamate SI spacer with a tertiary amine handle which strongly accelerates the spacer cyclization to give a bicyclic urea and the free hydroxy groups

of either cytotoxic (Camptothecin) or immunostimulatory (Resiquimod) drugs. *In silico* conformational analysis and  $pK_a$  calculations suggest a plausible mechanism for the superior efficacy of the advanced SI spacer compared to state-of-art analogues.

## Introduction

The selective delivery of drugs to the site of disease represents a widely pursued research goal, aimed at improving the efficacy and tolerability of pharmacological interventions. In this context, the covalent conjugation of pharmaceutical ingredients to antibodies (resulting in Antibody-Drug Conjugates, ADCs) represents one of the most validated technologies.<sup>[1]</sup> Historically, ADCs have been developed to release cytotoxic agents at the tumour site and kill cancer cells selectively, sparing healthy tissues. More recently, the ADC technology was adapted to various classes of pharmaceutical agents, including antibacterial,<sup>[2]</sup> anti-inflammatory,<sup>[3]</sup> and pro-inflammatory drugs.<sup>[4]</sup> In addition to antibodies, the covalent drug conjugation to different carriers (e.g. albumin,<sup>[5]</sup> peptides,<sup>[6]</sup> small ligands,<sup>[7]</sup> polymers,<sup>[8]</sup> etc.) is pushing the boundaries of targeted medicine. In most of these constructs, therapeutic effects are only displayed when the drug is effectively disconnected from the carrier. In this mechanism of action, a key role is played by the so-called self-immolative (SI) spacers, i.e. synthetic devices designed to undergo spontaneous disassembly in response to specific stimuli.<sup>[9]</sup> In particular, different types of activation

signals (see "Trigger Activation" in Figure 1) typically lead to the liberation of a reactive functional group in the SI spacer. The latter initiates a variety of intramolecular reactions (mainly electronic cascade in aromatic and  $\pi$ -extended systems<sup>[10]</sup> or cyclization of nucleophilic groups)<sup>[11]</sup> that terminate with the release of thermodynamically-stable end-products (see "SI spacer Degradation" in Figure 1).<sup>[12]</sup> In the prodrug context, not only SI spacers facilitate the drug disconnection from the carrier and its release in a pharmaceutically-active form, but they also act as chemical adaptors for the whole prodrug assembly.<sup>[13]</sup> Several conjugation strategies have been proposed to function-

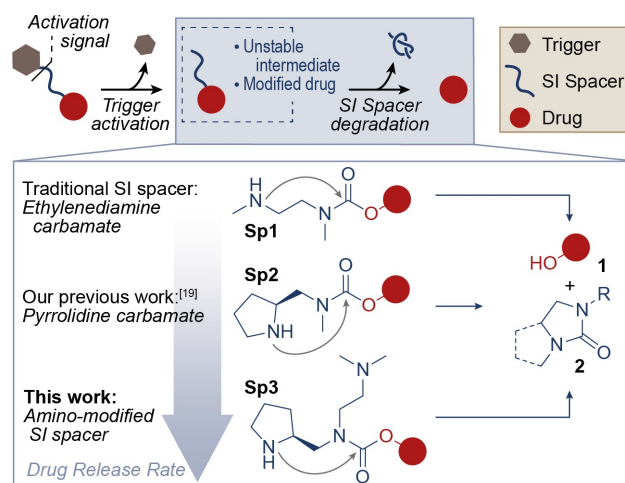


**Figure 1.** Schematic drug release mechanism of a generic covalent drug conjugate, consisting in the initial trigger activation and subsequent degradation of a self-immolative (SI) spacer. The molecular structure and degradation mechanism of three cyclizing amine-carbamate SI spacers (i.e. benchmark ethylenediamine-carbamate **Sp1**, pyrrolidine-carbamate **Sp2**<sup>[19]</sup> and its engineered derivative **Sp3**, described in this work) is shown: secondary amine cyclization leads to carbamate cleavage, to give the drug's free hydroxy group (**1**) and cyclic urea (**2** (mono-cyclic urea for **Sp1**, bicyclic urea for **Sp2/3**; R = Me for **Sp1/2**, R = (CH<sub>2</sub>)<sub>2</sub>NMe<sub>2</sub> for **Sp3**). SI spacer cyclization rates increase in the order **Sp1** < **Sp2** < **Sp3**.

[a] Dr. A. Dal Corso, M. Frigoli, M. Prevosti, M. Mason, Prof. L. Belvisi, Prof. L. Pignataro, Prof. C. Gennari  
Università degli Studi di Milano  
Dipartimento di Chimica  
via C. Golgi, 19, 20133 Milan (Italy)  
E-mail: alberto.dalcorso@unimi.it  
cesare.gennari@unimi.it

[b] Dr. R. Bucci  
Università degli Studi di Milano  
Dipartimento di Scienze Farmaceutiche  
via G. Venezian 21, 20133 Milan (Italy)

Supporting information for this article is available on the WWW under <https://doi.org/10.1002/cmdc.202200279>

© 2022 The Authors. ChemMedChem published by Wiley-VCH GmbH. This is an open access article under the terms of the Creative Commons Attribution License, which permits use, distribution and reproduction in any medium, provided the original work is properly cited.

alize a variety of bioactive molecules, including amines,<sup>[14]</sup> phenols,<sup>[15]</sup> primary<sup>[16]</sup> and secondary<sup>[17]</sup> alcohols. In particular, the use of carbamate bonds is a practical and versatile strategy to connect a variety of hydroxy payloads to specific triggers and the ethylenediamine-carbamate spacer (**Sp1**, Figure 1) has long represented a standard in drug conjugates and other stimuli-responsive systems.<sup>[18]</sup>

Our group has recently investigated the structural modification of **Sp1**. In 2020, we reported that the pyrrolidine-carbamate SI spacer **Sp2** (Figure 1) undergoes cyclative cleavage and releases OH-bearing drugs (**1**) and cyclic urea **2** at higher rates than **Sp1**. The incorporation of **Sp1** and **Sp2** into protease-activable anticancer prodrugs provided experimental evidence that a fast SI spacer degradation augments the anticancer effects *in vitro*.<sup>[19]</sup> In light of these data, we speculated that a rapid SI spacer degradation may be particularly important for the prodrug efficacy *in vivo*. Indeed, even if the trigger activation (Figure 1) occurs efficiently and selectively at the site of interest, a long timespan between this initial stimulus and the final drug release prolongs the drug survival in a modified and inactive form. This delayed activation would facilitate the drug migration from the site of disease, its excretion or, at worst, its activation in healthy organs.

We describe herein an advanced SI spacer (**Sp3** in Figure 1) in which a tertiary amine handle enables much faster cyclative drug release compared to previously described spacers of the same class. Thanks to this rapid carbamate cleavage, this accelerated spacer degradation holds promises for improved delivery of therapeutic agents.

## Results and Discussion

We undertook the structural optimization of the pyrrolidine-carbamate SI spacer **Sp2**, aimed at decreasing the carbamate half-life ( $t_{1/2}$ ) for a faster hydroxy cargo release. The molecular structures of the synthesized SI spacers are reported in Figure 2 (all synthetic procedures are reported in the Supporting Information). Here, the **Sp2** pyrrolidine ring was replaced by either a piperidine (in **Sp4**) or an isoxazolidine (in **Sp5**) cycle. In particular, **Sp4** was designed to assess the impact of the cyclic amine ring size on the SI spacer degradation.<sup>[20]</sup> On the other hand, the use of an isoxazolidine ring in **Sp5** aimed at evaluating the contribution of the "α-effect" to the spacer reactivity.<sup>[21]</sup> While **Sp4** was prepared starting from racemic 2-piperidinecarbaldehyde, the synthesis of **Sp5** was inspired by Bode's route to 5-oxaproline.<sup>[22]</sup> Moreover, as we recently observed the inhibitory effects on the spacer cyclization given by a phosphate monoester group,<sup>[23]</sup> we devised the SI spacer modification with a basic handle. Since at physiological pH (approximately 7.4) the pyrrolidine is mostly present as protonated species, a second amine handle may force the pyrrolidine deprotonation, thus lowering its  $pK_a$  value and increasing its nucleophilic character.<sup>[24]</sup> To this end, SI spacers **Sp3** and **Sp6/8** were endowed with a tertiary amine handle connected either at the carbamate N atom (in **Sp3** and **Sp7**) or at the pyrrolidine ring (in **Sp6** and **Sp8**). While the former

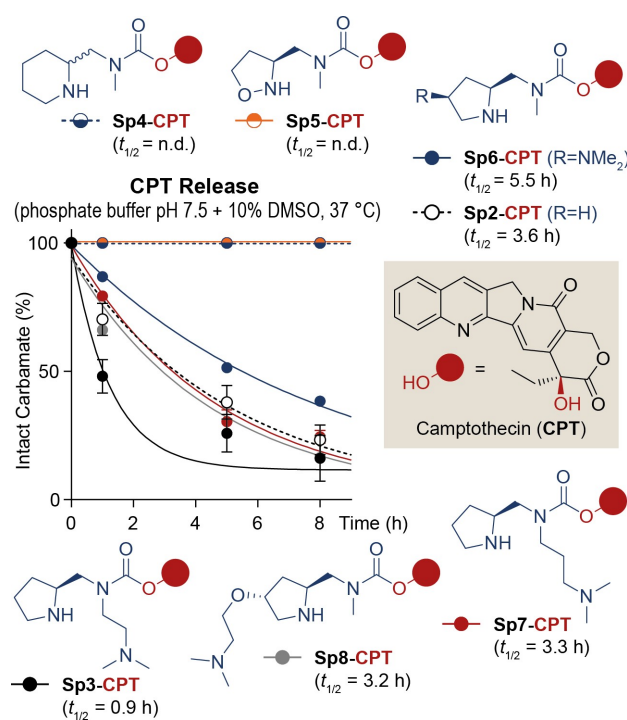


**Figure 2.** Molecular structure and drug release activity of II-generation cyclizing SI spacers (**Sp3/8**), connected to the tertiary hydroxy group of Camptothecin (CPT). Experimental procedures for the SI spacer-CPT module synthesis and release studies are included in the Supporting Information.

spacers were rapidly obtained by reductive amination of Boc-L-proline, the latter were prepared by multistep synthesis, starting from oxygenated proline derivatives, such as 4-oxo-L-proline and hydroxyproline. Firstly, the exocyclic secondary amine of SI spacers **Sp3/8** was conjugated to the tertiary hydroxy group of the anticancer drug Camptothecin (CPT) via carbamate bond. As described recently,<sup>[19,23]</sup> the final spacer-drug modules **Sp3/8-CPT** (Figure 2) were isolated as trifluoroacetate salts. These compounds were dissolved in a DMSO/phosphate buffer (pH 7.5) mixture and incubated at 37 °C, followed by aliquot collection at different time points and CPT release analysis by HPLC. The percentage of intact carbamate calculated from peak integrals was plotted versus time, and the spacer cyclization rates were estimated in terms of carbamate half-life ( $t_{1/2}$ ). The results of this first screening are summarized in Figure 2.

Notably, replacement of the native pyrrolidine ring with a piperidine (**Sp4**) and an isoxazolidine (**Sp5**) led to a complete inhibition of the cyclative carbamate cleavage.<sup>[25]</sup> On the other hand, the SI spacer derivatization with a tertiary amine led to some interesting results in terms of CPT release efficacy. In particular, carbamate **Sp6-CPT** released CPT with lower rates than reference **Sp2-CPT** ( $t_{1/2}$  = 5.5 and 3.6 h, respectively), while the reactivity of SI spacers **Sp7** ( $t_{1/2}$  = 3.3 h) and **Sp8** ( $t_{1/2}$  = 3.2 h) was slightly improved, but very similar to the one of native **Sp2**. To our delight, carbamate **Sp3-CPT** showed a half-life of 0.9 h, i.e. four times shorter than reference compound **Sp2-CPT**.<sup>[26]</sup> All in all, these data indicate that the cyclative cleavage of

pyrrolidine-carbamate SI spacers can be accelerated by a tertiary amine handle, provided that the latter is in close proximity to the electrophilic carbamate bond. Indeed, the tertiary amine installation in a remote position from the carbamate (e.g. in **Sp6** and **Sp8**) showed no significant impact on the CPT release rates compared to reference **Sp2**. The importance of the amine handle proximity is even more evident by considering the better CPT release performance of **Sp3** (where a C-2 alkyl chain connects the carbamate N atom to the tertiary amino group) compared to **Sp7** (bearing a C-3 alkyl chain).

With the aim at confirming the superior efficacy of the new SI spacer **Sp3**, we investigated its ability to release a different payload, namely the immunostimulatory drug Resiquimod (R848). This imidazoquinoline (IMD) is a potent agonist of Toll-like receptors (TLR) 7 and 8, intracellular proteins expressed by several types of immune cells and involved in the host defence from viral infections.<sup>[27]</sup>

By mimicking single-strand RNA fragments, IMDs induce TLR homodimerization and activate downstream pro-inflammatory pathways. Due to these pharmaceutical effects, tumour-targeted IMD prodrugs are being increasingly investigated to selectively activate the immune system at the site of disease, thus improving the outcomes of immunotherapy regimens.<sup>[4,28]</sup> As previously done with CPT, SI spacers **Sp1**, **Sp2** and **Sp3** were connected to the tertiary hydroxy group of R848 via carbamate bond. The resulting **Sp1/3-R848** adducts were dissolved in a DMSO/phosphate buffer (pH 7.5) mixture and incubated at 37 °C, following drug release analysis as described above. As shown by the HPLC traces and the chart in Figure 3, R848 carbamates proved generally more stable than the analogous CPT constructs. In particular, the native pyrrolidine spacer **Sp2** showed a very slow carbamate cleavage, with a half-life of 40 h calculated for the **Sp2-R848** construct. As expected, the drug release activity shown by **Sp2** was superior than the benchmark ethylenediamine-carbamate spacer **Sp1**, which released only traces of drug after eight-hour incubation. As observed with the CPT adducts, the tertiary amine-bearing spacer **Sp3** showed the highest drug release activity of the series, as the half-life of **Sp3-R848** carbamate ( $t_{1/2} = 7.6$  h) resulted approximately five times shorter than that of the **Sp2**-bearing analogue. In this experiment, LC-MS analysis of the **Sp3-R848** adduct upon eight-hour incubation confirmed the formation of bicyclic urea **2** during **Sp3** degradation (see Figure S1 in the Supporting Information). These CPT and R848 release data confirmed the superior performance of the advanced **Sp3** spacer compared to both **Sp2** and, even more dramatically, **Sp1** references.

To qualitatively investigate the structural basis for the **Sp3** spacer exceptional reactivity, we performed conformational analyses by computational methods of both **Sp2** and **Sp3** structures, connected to a generic alcohol (*tert*-butanol, "tBu") through a carbamate bond. In particular, Monte Carlo/Energy Minimization (MC/EM) conformational searches<sup>[29]</sup> were performed at the molecular mechanics level (OPLS3 force field)<sup>[30]</sup> on carbamates **Sp2-tBu** and **Sp3-tBu** in their main ionization state at pH 7.5, corresponding to positively-charged amino groups (i.e. protonated pyrrolidine in **Sp2-tBu**, protonated

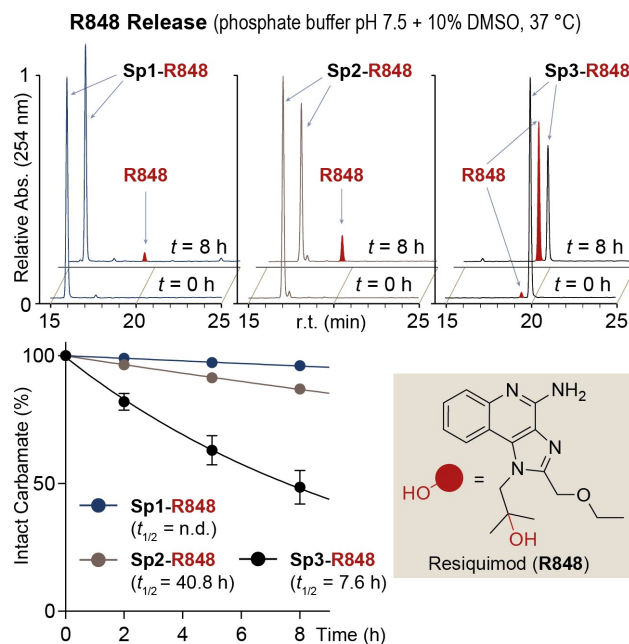


**Figure 3.** Drug release activity of SI spacers **Sp1/3**, connected to the tertiary hydroxy group of Resiquimod (R848). HPLC traces relative to the stability analysis of carbamates **Sp1/3-R848** at  $t = 0, 8$  h are shown (peak of free R848 is highlighted in red) together with stability curves. r.t.: retention time, Abs.: UV absorbance. Experimental procedures for the SI spacer-R848 carbamate synthesis and release studies are included in the Supporting Information.

pyrrolidine and tertiary amine in **Sp3-tBu**). Representative minimum-energy conformations selected from the molecular mechanics calculations were optimized at the DFT B3LYP/6-31G\* level of theory.<sup>[31]</sup> Solution phase energies of the obtained stationary points were computed at the same level of theory by single-point energy calculations including the water/PBF solvent model.<sup>[31]</sup> Finally,  $pK_a$  values of the protonated species were calculated on DFT minimum energy structures displaying the lowest solution phase energies. According to these calculations, carbamate **Sp2-tBu** adopts a preferential conformation (referred to as "**Sp2-tBu anti**" in Figure 4A) in which the pyrrolidinium ion engages the carbonyl  $sp^2$ -hybridized O atom in a hydrogen bond, forming a seven-membered ring. On the other hand, a similar intramolecular interaction of the pyrrolidinium ion with  $sp^3$ -hybridized O atom leads to the "**Sp2-tBu syn**" conformation, 2.74 kcal/mol higher in energy than the "**anti**" counterpart.

"**Anti**" rotamers in carbamates are typically favored over the "**syn**" counterparts by 1.0–1.5 kcal/mol,<sup>[32]</sup> and the 2.74 kcal/mol increased stability of "**Sp2-tBu anti**" versus "**Sp2-tBu syn**" indicates that rotational equilibrium of amine-carbamate modules can be dramatically influenced by intramolecular H bonding. Concerning **Sp3-tBu**, two simultaneous H bonds can be formed by two donors (i.e. pyrrolidinium and trialkyl ammonium ions), which can individually engage either O atoms (Figure 4A). In contrast to the **Sp2-tBu** data, the preferred **Sp3-tBu** conformation features the pyrrolidinium ion engaging the  $sp^3$ -hybridized O atom, whereas the  $sp^2$ -hybridized O atom binds the trialkyl ammonium ion. This "**Sp3-tBu syn**" conforma-

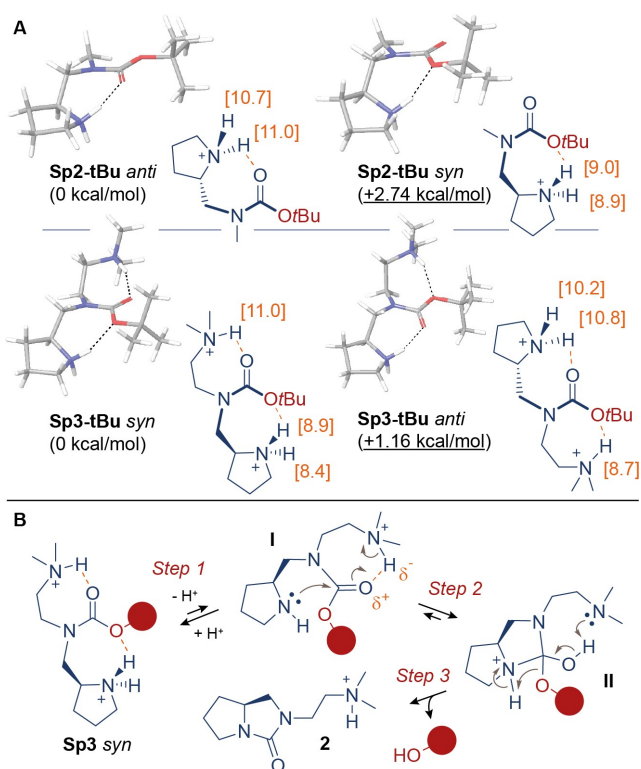


**Figure 4.** A) Molecular structures of representative conformations for Sp2/3-tBu, optimized at the DFT B3LYP/6-31G\* level. Relative energy differences are calculated from the corresponding solution phase energies (water PBF). Calculated  $pK_a$  values for N-H<sup>+</sup> protons are reported (orange). Additional conformations of Sp2/3-tBu are shown in Figure S2 in the Supporting Information. B) Plausible mechanism of carbamate cyclative cleavage carried out by SI spacer Sp3.

tion is favored by 1.16 kcal/mol over the “Sp3-tBu *anti*” counterpart, in which the pyrrolidinium and trialkyl ammonium ions engage the  $sp^2$ - and  $sp^3$ -hybridized O atoms, respectively (Figure 4, for additional conformations of Sp2-tBu and Sp3-tBu, see Figure S2 in the Supporting Information). Interestingly, the two pyrrolidinium protons in the “Sp3-tBu *syn*” conformation proved more acidic (calculated  $pK_a$  = 8.9, 8.4) than the trialkyl ammonium species ( $pK_a$  = 11.0).

These *in silico* data suggest a possible explanation for the observed SI spacer reactivity. Firstly, at the onset of SI spacer degradation, it is reasonable to assume that the nucleophilic attack of the uncharged pyrrolidine N atom to the carbonyl group occurs with a N–C–O bond angle  $>90^\circ$ , following the well-known Bürgi-Dunitz trajectory.<sup>[33]</sup> The three-dimensional analysis of the Sp-carbamate modules indicates that this geometry of attack is only accessible by the carbamate *syn* rotamers. Secondly, considering the perturbed  $pK_a$  of the pyrrolidinium ion in the “Sp3-tBu *syn*” structure, it is possible that the pyrrolidine nucleophilic attack in Sp3 is also facilitated by a preferential proton dissociation in aqueous medium.

In summary, the tertiary amine proximity to the carbamate group may facilitate the SI spacer degradation at different stages of the cyclization reaction, following the mechanism proposed in Figure 4B. In particular, upon pyrrolidine depro-

tonation (Step 1, equilibrium governed by the pH of the aqueous medium), the intramolecular hydrogen bond between the trialkylammonium ion and the  $sp^2$ -hybridized O atom in intermediate I may facilitate the pyrrolidine cyclization (Step 2) to give the tetrahedral intermediate II. Here, the basicity of the tertiary amine may favor the restoration of the  $sp^2$ -hybridized C center (bicyclic urea formation) and the liberation of the hydroxy group (Step 3). This impact of neighbouring groups on bond cleavage kinetics is reminiscent of “catalytic triads” in the active site of hydrolytic enzymes,<sup>[34]</sup> which have inspired the development of synthetic enzyme mimics.<sup>[35]</sup> Similarly, a positively-charged lysine  $\epsilon$ -amine group in an ADC construct was recently found to act as acid-catalyst, and exploited to induce modifications of acetal and succinimide labels connected to the antibody core.<sup>[36]</sup>

## Conclusions

The present work describes a highly reactive pyrrolidine-carbamate SI spacer (Sp3) in which a superfast carbamate cyclative cleavage is induced by the presence of a tertiary amine handle in close proximity to the carbamate bond. This advanced spacer showed better performance than Sp2 in the release of both the cytotoxic agent CPT and immunostimulatory drug R848. *In silico* conformational analysis and  $pK_a$  calculations allowed us to propose a plausible rationale for the superior efficacy of the advanced SI spacer compared to reference Sp2. Considering the very slow R848 release observed with state-of-art SI spacers Sp1 and Sp2, the new spacer Sp3 may be pivotal for the design of cleavable R848 conjugates, alternative to previous strategies for IMD derivatization.<sup>[37]</sup> Moreover, as we reported for the Sp2 reference,<sup>[19,23]</sup> the Sp3 module can be easily installed into functional drug delivery systems. For instance, the Sp3 connection to a *para*-aminobenzyl carbamate (PABC) spacer will access to protease-activable prodrugs, which represent the backbone of drug delivery technologies, including marketed ADCs.<sup>[38]</sup> In general, Sp3 application in different types of stimuli-responsive materials can be envisioned as a valid alternative to current strategies for hydroxyl cargo delivery.<sup>[13,16,17]</sup>

## Acknowledgements

We gratefully acknowledge Ministero dell'Università e della Ricerca (PRIN 2020 project 2020833Y75) for financial support. Mass spectrometry analyses were performed at the MS facility of the Unitech COSPECT at the University of Milan (Italy). Open Access funding provided by Università degli Studi di Milano within the CRUI-CARE Agreement.

## Conflict of Interest

The authors declare no conflict of interest.

## Data Availability Statement

The data that support the findings of this study are available in the supplementary material of this article.

**Keywords:** cascade reactions · disassembly · drug delivery · prodrugs · self-immolative spacers

- [1] C. Ceci, P. M. Lecal, G. Graziani, *Pharmacol. Ther.* **2022**, *236*, 108106.
- [2] S. Mariathan, M. W. Tan, *Trends Mol. Med.* **2017**, *23*, 135–149.
- [3] a) A. Han, O. Olsen, C. D'Souza, J. Shan, F. Zhao, J. Yanolatos, Z. Hovhannisyian, S. Haxhinasto, F. Delfino, W. Olson, *J. Med. Chem.* **2021**, *64*, 11958–11971; b) A. D. Hobson, M. J. McPherson, W. Waegell, C. A. Goess, R. H. Stoffel, X. Li, J. Zhou, Z. Wang, Y. Yu, A. Hernandez Jr., S. H. Bryant, S. L. Mathieu, A. K. Bischoff, J. Fitzgibbons, M. Pawlikowska, S. Puthenveetil, L. C. Santora, L. Wang, L. Wang, C. C. Marvin, M. E. Hayes, A. Shrestha, K. A. Sarris, B. Li, *J. Med. Chem.* **2022**, *65*, 4500–4533.
- [4] S. E. Ackerman, C. I. Pearson, J. D. Gregorio, J. C. Gonzalez, J. A. Kenkel, F. J. Hartmann, A. Luo, P. Y. Ho, H. LeBlanc, L. K. Blum, S. C. Kimmey, A. Luo, M. L. Nguyen, J. C. Paik, L. Y. Sheu, B. Ackerman, A. Lee, H. Li, J. Melrose, R. P. Laura, V. C. Ramani, K. A. Henning, D. Y. Jackson, B. S. Safina, G. Yonehiro, B. H. Devens, Y. Carmi, S. J. Chapin, S. C. Bendall, M. Kowanetz, D. Dornan, E. G. Engleman, M. N. Alonso, *Nat. Cancer* **2021**, *2*, 18–33.
- [5] a) R. Châtre, J. Lange, E. Péraudeau, P. Poinot, S. Lerondel, A. Le Pape, J. Clarhaut, B. Renoux, S. Papot, *J. Controlled Release* **2020**, *327*, 19–25; b) Y. Huang, L. Wang, Z. Cheng, B. Yang, J. Yu, Y. Chen, W. Lu, *J. Controlled Release* **2021**, *339*, 297–306.
- [6] B. M. Cooper, J. Iegre, D. H. O' Donovan, M. Ölwegård Halvarsson, D. R. Spring, *Chem. Soc. Rev.* **2021**, *50*, 1480–1494.
- [7] a) S. Cazzamalli, A. Dal Corso, F. Widmayer, D. Neri, *J. Am. Chem. Soc.* **2018**, *140*, 1617–1621; b) T. Kumar Patel, N. Adhikari, S. A. Amin, S. Biswas, T. Jha, B. Ghosh, *New J. Chem.* **2021**, *45*, 5291–5321.
- [8] I. Ekladios, Y. L. Colson, M. W. Grinstaff, *Nat. Rev. Drug Discovery* **2019**, *18*, 273–294.
- [9] A. Alouane, R. Labruère, T. Le Saux, F. Schmidt, L. Jullien, *Angew. Chem. Int. Ed.* **2015**, *54*, 7492–7509; *Angew. Chem.* **2015**, *127*, 7600–7619.
- [10] a) S. Gnaïm, D. Shabat, *Acc. Chem. Res.* **2014**, *47*, 2970–2984; b) D. A. Roberts, B. S. Pilgrim, T. N. Dell, M. M. Stevens, *Chem. Sci.* **2020**, *11*, 3713–3718; c) S. Davies, B. L. Oliveira, G. J. L. Bernardes, *Org. Biomol. Chem.* **2019**, *17*, 5725–5730; d) S. Huvelle, T. Le Saux, L. Jullien, F. Schmidt, *Org. Biomol. Chem.* **2022**, *20*, 240–246; e) D. A. Rose, J. W. Treacy, Z. J. Yang, J. Hoon Ko, K. N. Houk, H. D. Maynard, *J. Am. Chem. Soc.* **2022**, *144*, 6050–6058.
- [11] a) S. Huvelle, A. Alouane, T. Le Saux, L. Jullien, F. Schmidt, *Org. Biomol. Chem.* **2017**, *15*, 3435–3443; b) E. Procházková, P. Šimon, M. Straka, J. Filo, M. Majek, M. Cigáň, O. Basczyński, *Chem. Commun.* **2021**, *57*, 211–214; c) M. Ximenis, A. Sampedro, L. Martínez-Crespo, G. Ramis, F. Orvay, A. Costa, C. Rotger, *Chem. Commun.* **2021**, *57*, 2736–2739.
- [12] a) O. Shelef, S. Gnaïm, D. Shabat, *J. Am. Chem. Soc.* **2021**, *143*, 21177–21188; b) Q. E. A. Sirianni, E. R. Gillies, *Polymer* **2020**, *202*, 122638.
- [13] a) A. Dal Corso, L. Pignataro, L. Belvisi, C. Gennari, *Chem. Eur. J.* **2019**, *25*, 14740–14757; b) R. V. Gonzaga, L. A. do Nascimento, S. S. Santos, B. A. Machado Sanches, J. Giarolla, E. I. Ferreira, *J. Pharm. Sci.* **2020**, *109*, 3262–3281; c) R. Sheyi, B. G. de la Torre, F. Albericio, *Pharmaceutica* **2022**, *14*, 396.
- [14] J. Z. Hamilton, T. A. Pires, J. A. Mitchell, J. H. Cochran, K. K. Emmerton, M. Zaval, I. J. Stone, M. E. Anderson, S. Jin, A. B. Waight, R. P. Lyon, P. D. Senter, S. C. Jeffrey, P. J. Burke, *ChemMedChem* **2021**, *16*, 1077–1081.
- [15] S. Park, S. Y. Kim, J. Cho, D. Jung, D. Seo, J. Lee, S. Lee, S. Yun, H. Lee, O. Park, B. Seo, S. Kim, M. Seol, S. H. Woo, T. K. Park, *Bioconjugate Chem.* **2019**, *30*, 1969–1978.
- [16] a) J. C. Kern, D. Dooney, R. Zhang, L. Liang, P. E. Brandish, M. Cheng, G. Feng, A. Beck, D. Bresson, J. Firdos, D. Gately, N. Knudsen, A. Manibusan, Y. Sun, R. M. Garbaccio, *Bioconjugate Chem.* **2016**, *27*, 2081–2088; b) K. Yonesaka, N. Takegawa, S. Watanabe, K. Haratani, H. Kawakami, K. Sakai, Y. Chiba, N. Maeda, T. Kagari, K. Hirotsu, K. Nishio, K. Nakagawa, *Oncogene* **2019**, *38*, 1398–1409.
- [17] R. V. Kolakowski, K. T. Haelsig, K. K. Emmerton, C. I. Leiske, J. B. Miyamoto, J. H. Cochran, R. P. Lyon, P. D. Senter, S. C. Jeffrey, *Angew. Chem. Int. Ed.* **2016**, *55*, 7948–7951; *Angew. Chem.* **2016**, *128*, 8080–8083.
- [18] a) For an early report on the Sp1 spacer, see: W. S. Saari, J. E. Schwering, P. A. Lyle, S. J. Smith, E. L. Engelhardt, *J. Med. Chem.* **1990**, *33*, 97–101; b) Sp1 spacer proved active at releasing phenols, secondary and tertiary alcohols, but proved inefficient in the case of primary alcohols, see ref. 16a.
- [19] A. Dal Corso, V. Borlandelli, C. Corno, P. Perego, L. Belvisi, L. Pignataro, C. Gennari, *Angew. Chem. Int. Ed.* **2020**, *59*, 4176–4181; *Angew. Chem.* **2020**, *132*, 4205–4210.
- [20] For a cyclizing amine-carbamate SI spacer where the piperidine endocyclic N atom was connected to a phenolic leaving group, see: O. Thorn-Seshold, M. Vargas-Sanchez, S. McKeon, J. Hasserodt, *Chem. Commun.* **2012**, *48*, 6253–6255.
- [21] The  $\alpha$ -effect was described as the enhanced reactivity of nucleophiles bearing an unshared pair of electrons at the atom adjacent to the nucleophilic centre, see T. A. Nigst, A. Antipova, H. Mayr, *J. Org. Chem.* **2012**, *77*, 8142–8155.
- [22] C. E. Murar, T. J. Harmand, J. W. Bode, *Bioorg. Med. Chem.* **2017**, *25*, 4996–5001.
- [23] A. Dal Corso, S. Arosio, N. Arrighetti, P. Perego, L. Belvisi, L. Pignataro, C. Gennari, *Chem. Commun.* **2021**, *57*, 7778–7781.
- [24]  $pK_a$  perturbation is typically observed in proteins, where hyper-reactive nucleophilic residues are fundamental for the catalytic activity of enzymes (see T. K. Harris, G. J. Turner, *IUBMB Life* **2002**, *53*, 85–98), or represent preferential sites for the protein modification with electrophilic species (see: J. Pettinger, K. Jones, M. D. Cheeseman, *Angew. Chem. Int. Ed.* **2017**, *56*, 15200–15209; *Angew. Chem.* **2017**, *129*, 15398–15408).
- [25] The stability of carbamate Sp4-CPT may be ascribed to a suboptimal conformation of the piperidine spacer compared to the native pyrrolidine. For instance, pyrrolidine and piperidine rings exhibit different degrees of N atom pyramidalization (see: T. Schnitzer, J. S. Mohler, H. Wennemers, *Chem. Sci.* **2020**, *11*, 1943–1947). As for carbamate Sp5-CPT, this construct proved partially insoluble in the 9:1 aqueous buffer/DMSO mixture, differently from all other carbamates in the series. This observation indicates that the  $\alpha$ -oxygen atom effectively reduces both the N basicity (leading to a poorly soluble uncharged species at pH 7.5) and its nucleophilic character. The stability of Sp5-CPT was also analysed in a phosphate buffer solution at pH 7.5, with DMSO content increased to 20% DMSO. In this case, the compound was perfectly soluble, but still no CPT release was observed.
- [26] The release of free CPT was also studied upon Sp2-CPT and Sp3-CPT incubation under more acidic conditions (acetate buffer, pH 5), mimicking the lysosomal compartment. Although under these conditions both carbamates proved much more stable, Sp3 showed consistently higher drug release activity than the Sp2 reference.
- [27] S. Bhagchandani, J. A. Johnson, D. J. Irvine, *Adv. Drug Delivery Rev.* **2021**, *175*, 113803.
- [28] a) B. Wang, S. Van Herck, Y. Chen, X. Bai, Z. Zhong, K. Deswarte, B. N. Lambrecht, N. N. Sanders, S. Lienenklaus, H. W. Scheeren, S. A. David, F. Kiessling, T. Lammers, B. G. De Geest, Y. Shi, *J. Am. Chem. Soc.* **2020**, *142*, 12133–12139; b) E. Bolli, M. Scherger, S. M. Arnouk, A. R. Pombo Antunes, D. Straßburger, M. Urschbach, J. Stickdorn, K. De Vlamincq, K. Movahedi, H. J. Räder, S. Hernot, P. Besenius, J. A. Van Ginderachter, L. Nuhn, *Adv. Sci.* **2021**, *8*, 2004574; c) B. J. Ignacio, T. J. Albin, A. P. Esser-Kahn, M. Verdoes, *Bioconjugate Chem.* **2018**, *29*, 587–603.
- [29] a) G. Chang, W. C. Guida, W. C. Still, *J. Am. Chem. Soc.* **1989**, *111*, 4379–4386; b) MacroModel, version 11.1, Schrödinger, LLC, New York, NY, **2016**.
- [30] K. Roos, C. Wu, W. Damm, M. Reboul, J. M. Stevenson, C. Lu, M. K. Dahlgren, S. Mondal, W. Chen, L. Wang, R. Abel, R. A. Friesner, E. D. Harder, *J. Chem. Theory Comput.* **2019**, *15*, 1863–1874.
- [31] Jaguar, version 9.1, release 14, Schrödinger, Schrödinger Suite LLC, New York, NY, **2016**.
- [32] A. L. Moraczewski, L. A. Banaszynski, A. M. From, C. E. White, B. D. Smith, *J. Org. Chem.* **1998**, *63*, 7258–7262.
- [33] For an analysis of the Bürgi-Dunitz trajectory (107°) impact on the efficacy of covalent enzyme inhibitors bearing carbamate groups, see M. Mileni, S. Kamtekar, D. C. Wood, T. E. Benson, B. F. Cravatt, R. C. Stevens, *J. Mol. Biol.* **2010**, *400*, 743–754.
- [34] G. Dodson, A. Wlodawer, *Trends Biochem. Sci.* **1998**, *23*, 347–352.
- [35] M. D. Nothing, Z. Xiao, A. Bhaskaran, M. T. Blyth, C. W. Bennett, M. L. Coote, L. A. Connal, *ACS Catal.* **2019**, *9*, 168–187.

- [36] X. Ferhati, E. Jiménez-Moreno, E. A. Hoyt, G. Salluce, M. Cabeza-Cabrero, C. D. Navo, I. Compañón, P. Akkapeddi, M. J. Matos, N. Salaverri, P. Garrido, A. Martínez, V. Laserna, T. V. Murray, G. Jiménez-Osés, P. Ravn, G. J. L. Bernardes, F. Corzana, *J. Am. Chem. Soc.* **2022**, *144*, 5284–5294.
- [37] For the use of the **Sp1-R848** carbamate in tumour-targeted conjugates, see: Ni. Keen, K. McDonnell, P. U. Park, G. E. Mudd, G. Ivanova-Berndt, Bicyclic peptide ligands PRR-A conjugates and uses thereof, Bicycle, PCT/GB2018/052310, **2018**. For R848 modification at the aniline group, see: K. A. Ryu, L. Stutts, J. K. Tom, R. J. Mancini, A. P. Esser-Kahn, *J. Am. Chem. Soc.* **2014**, *136*, 10823–10825. For the conjugation of the R848 tertiary alcohol through hydrolysable ester bond, see: R. Lu, C. Groer, P. A. Kleindl, K. R. Moulder, A. Huang, J. R. Hunt, S. Cai, D. J. Aires, C. Berkland, M. Laird Forrest, *J. Controlled Release* **2019**, *306*, 165–176. For
- IMD conjugates assembled through uncleavable bonds, see Refs. 4, 28b and L. Nuhn, N. Vanparijs, A. De Beuckelaer, L. Lybaert, G. Verstraete, K. Deswarte, S. Lienenklaus, N. M. Shukla, A. C. D. Salyer, B. N. Lambrecht, J. Grooten, S. A. David, S. De Koker, B. G. De Geest, *Proc. Natl. Acad. Sci. USA* **2016**, *113*, 8098–8103.
- [38] R. Walther, J. Rautio, A. N. Zelikin, *Adv. Drug Delivery Rev.* **2017**, *118*, 65–77.

---

Manuscript received: May 20, 2022  
Accepted manuscript online: May 27, 2022  
Version of record online: June 14, 2022

# ChemMedChem

Supporting Information

## **Advanced Pyrrolidine-Carbamate Self-Immolative Spacer with Tertiary Amine Handle Induces Superfast Cyclative Drug Release**

Alberto Dal Corso,\* Margaux Frigoli, Martina Prevosti, Mattia Mason, Raffaella Bucci, Laura Belvisi, Luca Pignataro, and Cesare Gennari\*

# Supporting Information

## Table of Contents

<b>Supplementary Figures</b>	<b>S2</b>
<b>Materials and Methods</b>	<b>S3</b>
<b>List of Abbreviations and Symbols</b>	<b>S4</b>
<b>Synthetic procedures</b>	<b>S5</b>
General Procedures	S5
Synthesis of Sp3-CPT	S6
Synthesis of Sp4-CPT	S7
Synthesis of Sp5-CPT	S8
Synthesis of Sp6-CPT	S10
Synthesis of Sp7-CPT	S13
Synthesis of Sp8-CPT	S14
Synthesis of Sp1-R848, Sp2-R848, Sp3-R848	S19
<b>Carbamate Cleavage Studies</b>	<b>S24</b>
Experimental Procedure for Sp-CPT Modules	S24
Experimental Procedure for Sp-R848 modules	S25
<b>Computational Studies</b>	<b>S26</b>
<b>Appendix</b>	<b>S28</b>
HPLC Data – Sp-CPT Modules	S28
HPLC Data – Sp-R848 Modules	S35
NMR Spectra	S38



## Supplementary Figures

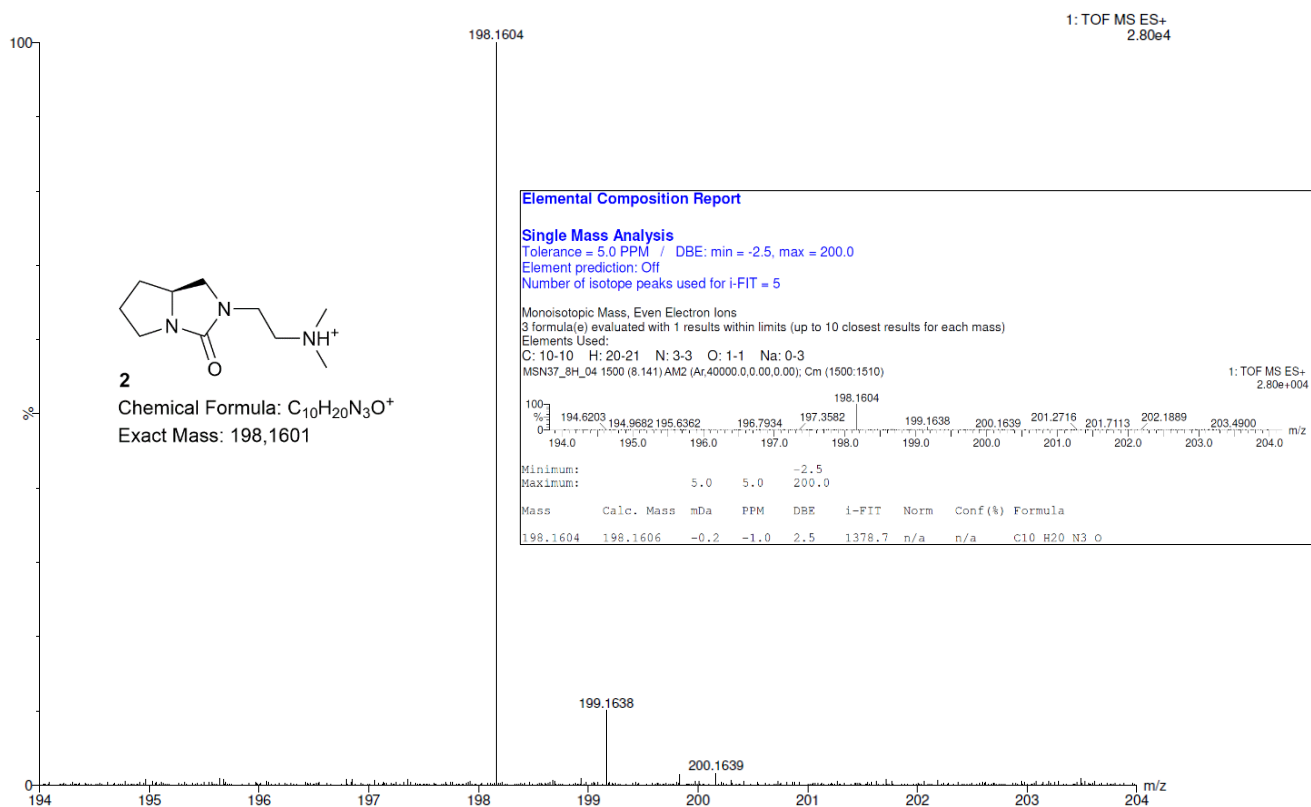


**Figure S1.** HRMS spectrum and elemental composition report for bicyclic urea **2** (**Sp3** cyclization end-product) detected by LC-MS analysis of **Sp3-R848** upon incubation for 8 h in phosphate buffer.

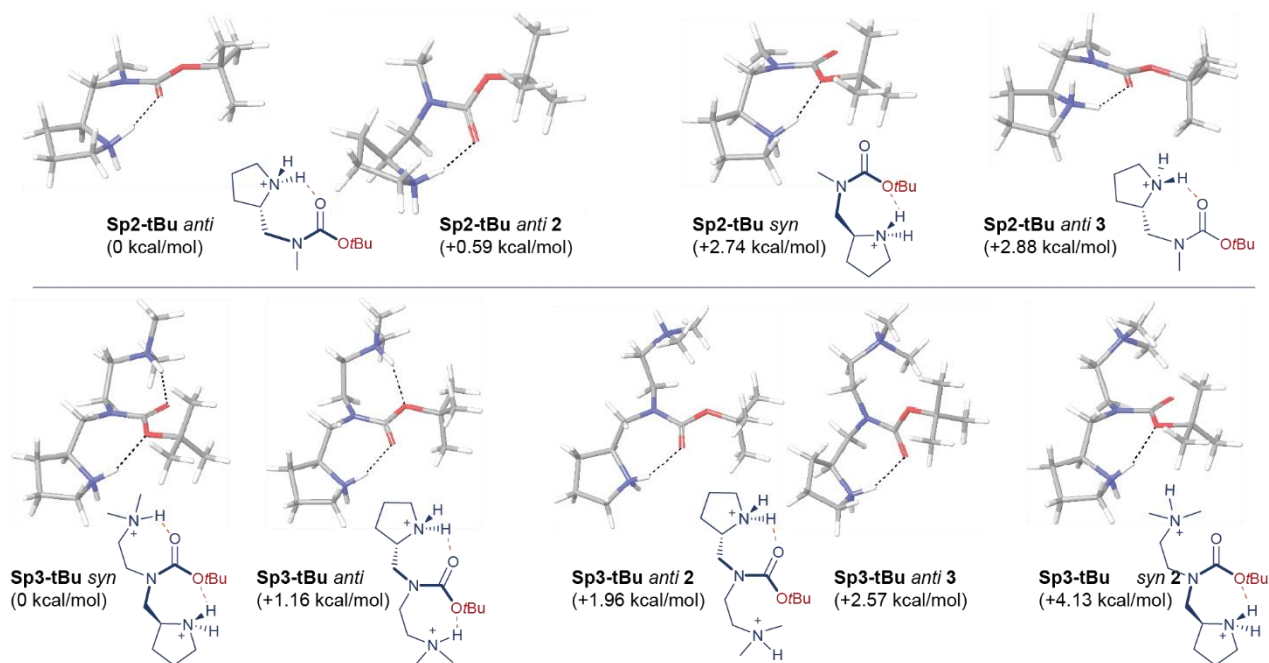


**Figure S2.** Molecular structures of representative conformations for **Sp2/3-tBu**, optimized at the DFT B3LYP/6-31G\* level. Relative energy differences are calculated from the corresponding solution phase energies (water PBF).

## **Materials and Methods**

All manipulations requiring anhydrous conditions were carried out in flame-dried glassware, with magnetic stirring and under a nitrogen atmosphere. All commercially available reagents were used as received. Anhydrous solvents were purchased from commercial sources and withdrawn from the container by syringe, under a slight positive pressure of nitrogen. The reactions were monitored by analytical thin-layer chromatography (TLC) using silica gel 60 F254 pre-coated glass plates (0.25 mm thickness). Visualization was accomplished by irradiation with a UV lamp and/or staining with a ceric ammonium molybdate solution, 2,4-dinitrophenylhydrazine, concentrated H<sub>2</sub>SO<sub>4</sub> or ninhydrin. Flash column chromatography was performed according to the method of Still and co-workers<sup>1</sup> using Chromagel 60 ACC (40-63 μm) silica gel. Proton chemical shifts are reported in ppm (δ) with the solvent reference relative to tetramethylsilane (TMS) employed as the internal standard (CDCl<sub>3</sub> δ = 7.26 ppm; CD<sub>2</sub>Cl<sub>2</sub>, δ = 5.32 ppm; d<sub>6</sub>-DMSO, δ = 2.50 ppm; CD<sub>3</sub>OD, δ = 3.33 ppm, d<sub>8</sub>-THF δ = 3.58 ppm, 1.73 ppm). The following abbreviations are used to describe spin multiplicity: s = singlet, d = doublet, t = triplet, q = quartet, m = multiplet, bs = broad signal, dd = doublet of doublet. Carbon NMR spectra were recorded on a spectrometer operating at 100.63 MHz, with complete proton decoupling. Carbon chemical shifts are reported in ppm (δ) relative to TMS with the respective solvent resonance as the internal standard (CDCl<sub>3</sub>, δ = 77.16 ppm; CD<sub>2</sub>Cl<sub>2</sub>, δ = 54.00 ppm; d<sub>6</sub>-DMSO, δ = 39.51 ppm; CD<sub>3</sub>OD, δ = 49.05 ppm; d<sub>8</sub>-THF δ = 67.57 ppm, 25.37 ppm). HPLC purifications were performed on Dionex Ultimate 3000 equipped with Dionex RS Variable Wavelength Detector (column: Atlantis Prep T3 OBDTM 5 μm 19 x 100 mm; flow 10 ml/min unless stated otherwise). HPLC analysis of carbamate stability was performed on a Waters 515 HPLC pumps equipped with 996 photodiode array detector and Waters Atlantis T3 - 5 μm - 4.6 x 100 mm column (injection volume: 200 μL) and on a Jasco LC-4000 HPLC System equipped with MD-4010 photodiode array detector and Phenomenex Gemini-NX 5 μm - 4.6 x 150 mm column (injection volume: 20 μL). High-resolution mass spectrometry analysis (HRMS, 4 decimal places) were performed on a Q-TOF Synapt G2-Si instrument available at the MS facility of the Unitech COSPECT at the University of Milan. Low resolution mass spectra (MS, 1 and 2 decimal places) were recorded on a Thermo Scientific LCQ Fleet Ion Trap Mass Spectrometer (ESI source). Camptothecin carbonate **CPT-PNP**<sup>2</sup>, Boc-Hyp-OMe,<sup>3</sup> and **Sp2-CPT**<sup>4</sup> were prepared following published procedures.

---

1 W. C. Still, M. Kahn, A. Mitra, *J. Org. Chem.* 1978, **43**, 2923.

2 E. Riva, D. Comi, S. Borrelli, F. Colombo, B. Danieli, J. Borlak, L. Evensen, J. B. Lorens, G. Fontana, O. M. Gia, L. Dalla Via D. Passarella, *Bioorg. Med. Chem.* 2010, **18**, 8660.

3 K. K. Schumacher, J. Jiang, M. M. Joullié, *Tetrahedron: Asymmetry* 1998, **17**, 47.

4 A. Dal Corso, V. Borlandelli, C. Corno, P. Perego, L. Belvisi, L. Pignataro, C. Gennari, *Angew. Chem. Int. Ed.* 2020, **59**, 4176.

### List of Abbreviations and Symbols

AcOEt	Ethyl Acetate	Me	Methyl
AcOH	Acetic acid	MeCN	Acetonitrile
aq.	Aqueous solution	MeOH	Methanol
Boc	Tert-butyloxycarbonyl-	min.	Minutes
DIBAL-H	Diisobutylaluminum hydride	MS	Mass Spectroscopy
DIPEA	<i>N,N</i> -Diisopropylethylamine	MW	Molecular weight
DMAP	4-Dimethylaminopyridine	NMR	Nuclear Magnetic Resonance
DMF	Dimethylformamide	NMO	4-Methylmorpholine N-oxide
DMP	Dess-Martin periodinane	ppm	Part per million
DMSO	Dimethylsulfoxide	r.t.	Room temperature
equiv.	Equivalents	$R_f$	Retention factor
ESI	Electrospray ionization	sat.	Saturated
Et	Ethyl	<i>t</i> Bu	<i>tert</i> -Butyl
h	Hours	<i>tert</i>	Tertiary
Hex	<i>n</i> -Hexane	TEA	Triethylamine
HPLC	High performance liquid chromatography	TFA	Trifluoroacetic acid
HRMS	High resolution mass spectroscopy	THF	Tetrahydrofuran
Hyp	(2 <i>S</i> ,4 <i>R</i> )-4-Hydroxyproline	$t_R$	Retention time
$J$	Scalar coupling constants	$\delta$	Chemical shift
KHMDS	Potassium hexamethyldisilazide		

## Synthetic procedures

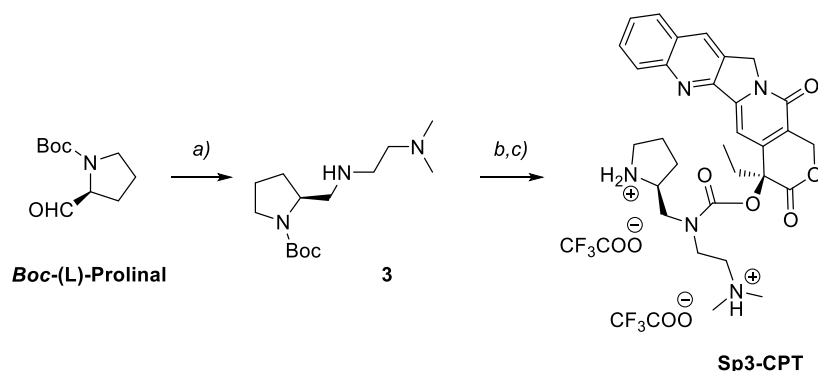
### General Procedures

**General procedure A for partial reduction of L-Proline esters.** Ester (1 equiv.) was dissolved in dry  $\text{CH}_2\text{Cl}_2$  (0.2 M), stirred under nitrogen atmosphere, and cooled at  $-78\text{ }^\circ\text{C}$  with an acetone/dry ice bath. DIBAL-H (1 M in hexane, 1 equiv.) was slowly added to the solution and the mixture was stirred at  $-78\text{ }^\circ\text{C}$  until starting material consumption was detected by TLC. Later on, MeOH was added at  $-78\text{ }^\circ\text{C}$  (3 x 30  $\mu\text{L}$ ) and the solution was stirred for 5 minutes. The mixture was warmed to r.t. and transferred into a separatory funnel containing a sat. aqueous  $\text{NH}_4\text{Cl}$  solution (25 mL). The solution was extracted with  $\text{CH}_2\text{Cl}_2$  (3 x 30 mL), dried and concentrated in vacuum. Unless stated otherwise, the resulting aldehyde was used in the following synthetic step without further purification.

**General procedure B for reductive amination.** Aldehyde (1 equiv.) was dissolved in  $\text{CH}_2\text{Cl}_2/\text{AcOH}$  under nitrogen atmosphere. Primary amine (4 equiv.) and  $\text{NaBH}(\text{OAc})_3$  (5 equiv.) were added to the aldehyde solution and the reaction was stirred at r.t. overnight. The mixture was transferred into a separatory funnel and diluted with  $\text{CH}_2\text{Cl}_2$  (10 mL). A 10%  $\text{Na}_2\text{CO}_3$  solution (20 mL) was added and the stirring mixture was flushed with nitrogen.  $\text{NaOH}$  2 M was then added until pH  $\sim 12$ . The mixture was extracted with  $\text{CH}_2\text{Cl}_2$  (3 x 25 mL). Collected organic phases were washed with brine (1 x 5 mL), dried and concentrated under vacuum.

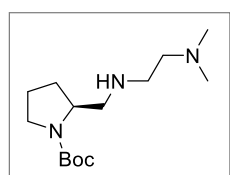
**General procedure C for Boc deprotection.** To an ice-cold  $\text{CH}_2\text{Cl}_2$  solution of the *N*-Boc-protected compound, half volume of TFA was added dropwise at  $0\text{ }^\circ\text{C}$  and the mixture was stirred at r.t. for 1 h. The solvent was evaporated and then  $\text{CH}_2\text{Cl}_2$  was added for two times to the residue followed by evaporation under vacuum, to afford the amine TFA salt.

## Synthesis of Sp3-CPT



**Scheme S1.** REAGENTS AND CONDITIONS: a) *N,N*-dimethylethylenediamine, NaBH(OAc)<sub>3</sub>, AcOH in dry CH<sub>2</sub>Cl<sub>2</sub>, r.t., overnight; b) CPT-PNP, dry CH<sub>2</sub>Cl<sub>2</sub>, r.t. 3h; c) TFA/CH<sub>2</sub>Cl<sub>2</sub> 1:2, 0 °C to r.t., 45 min.

### *Tert*-butyl (*S*)-2-(((2-(dimethylamino)ethyl)amino)methyl)pyrrolidine-1-carboxylate (**3**)

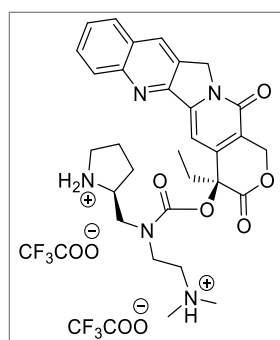


C<sub>14</sub>H<sub>29</sub>N<sub>3</sub>O<sub>2</sub>  
MW: 271.41 g · mol<sup>-1</sup>

Boc-(L)-Prolinal (186 μL, 1 mmol, 1 equiv.) was dissolved in CH<sub>2</sub>Cl<sub>2</sub>/AcOH (20 + 2 mL) under nitrogen atmosphere and treated with *N,N*-dimethylethylenediamine (95% wt, 438 μL, 4 mmol, 4 equiv.) following General Procedure B. The crude product was purified with column chromatography (gradient from 10% to 20% MeOH in CH<sub>2</sub>Cl<sub>2</sub>) to give amine **3** (232 mg, quant) as a colourless oil.

<sup>1</sup>H NMR (400 MHz, MeOD) δ 3.89 (bs, 1H), 3.39-3.28 (m, 2H), 2.87-2.67 (m, 3H), 2.59 (m, 1H), 2.53-2.41 (m, 2H), 2.27 (s, 6H), 2.04-1.77 (m, 4H), 1.47 (s, 9H) ppm; MS (ESI): *m/z* calcd. for [C<sub>14</sub>H<sub>29</sub>N<sub>3</sub>O<sub>2</sub>]<sup>+</sup>: 272.23 [M+H]<sup>+</sup>, found: 272.29.

### Sp3-CPT



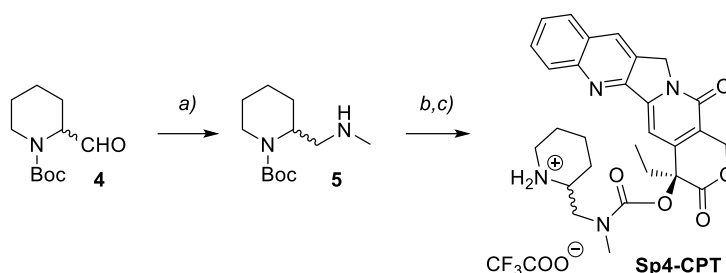
C<sub>30</sub>H<sub>35</sub>N<sub>5</sub>O<sub>5</sub>  
MW: 545.64 g · mol<sup>-1</sup> + TFA

To a solution of CPT-PNP (9 mg, 17 μmol, 1 equiv.) in dry CH<sub>2</sub>Cl<sub>2</sub> was added compound **3** (13.6 mg, 50 μmol, 3 equiv.) under nitrogen atmosphere followed by DIPEA (11.9 μL, 68 μmol, 4 equiv.). The reaction

was stirred at 25 °C for 2h. The crude product [ $R_f = 0.40$  (9:1  $\text{CH}_2\text{Cl}_2/\text{MeOH}$ )] was dissolved in dry  $\text{CH}_2\text{Cl}_2$  (600  $\mu\text{L}$ , 0.05 M) and treated following General Procedure C. The crude product was then purified by HPLC (eluent A:  $\text{H}_2\text{O} + 0.1\%$  TFA; eluent B: MeCN, ramp from 0% B (at min 1) to 60% B (at min 10.5),  $t_R$  (product): 8.6 min). The purified product was lyophilized to give carbamate **Sp3-CPT** as a yellow solid (22 mg, 95%).

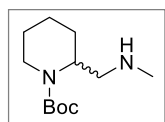
MS (ESI):  $m/z$  calcd. for  $[\text{C}_{30}\text{H}_{35}\text{N}_5\text{O}_5]^+$ : 546.27  $[M+H]^+$ , found: 546.48; HRMS (ESI)  $m/z$  calcd. for  $[\text{C}_{30}\text{H}_{35}\text{N}_5\text{O}_5]^+$ : 546.2716  $[M+H]^+$ , found: 546.2722.

## Synthesis of Sp4-CPT



**Scheme S2.** REAGENTS AND CONDITIONS: a)  $\text{MeNH}_2$ ,  $\text{NaBH}(\text{OAc})_3$  in dry  $\text{CH}_2\text{Cl}_2$ , r.t., overnight; b) **CPT-PNP**, dry  $\text{CH}_2\text{Cl}_2$ , r.t. 3h; c) TFA/ $\text{CH}_2\text{Cl}_2$  1:2, 0 °C to r.t., 45 min.

### Tert-butyl 2-((methylamino)methyl)piperidine-1-carboxylate (**5**)

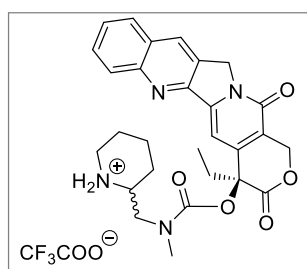


$\text{C}_{12}\text{H}_{24}\text{N}_2\text{O}_2$   
MW: 228.34  $\text{g} \cdot \text{mol}^{-1}$

1-*N*-Boc-2-piperidinecarbaldehyde (**4**) (racemate, 214 mg, 1 mmol, 1 equiv.) was dissolved in  $\text{CH}_2\text{Cl}_2/\text{AcOH}$  (20 + 2 mL) under nitrogen atmosphere and treated with methylamine (33% wt in absolute ethanol, 373.6  $\mu\text{L}$ , 3 mmol, 3 equiv.) following General Procedure B. Amine **5** was obtained as a colourless oil (100 mg, 45%).

$^1\text{H}$  NMR (400 MHz, MeOD)  $\delta$  4.35 (m, 1H), 3.96 (m, 1H), 2.88-2.82 (m, 2H), 2.64 (dd,  $J = 12.5, 6.6$  Hz, 1H), 2.39 (s, 3H), 1.70-1.56 (m, 6H), 1.46 (s, 9H) ppm.

### Sp4-CPT

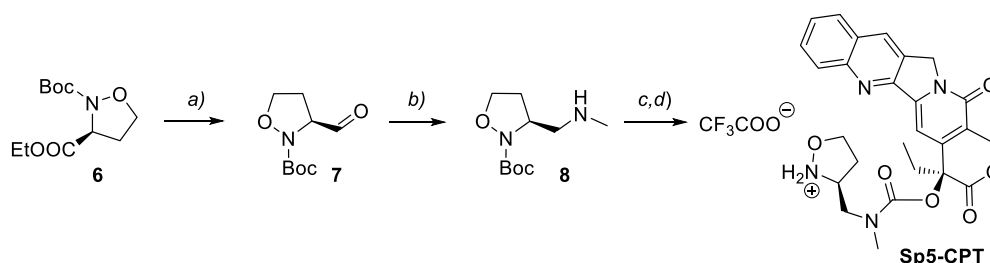


$\text{C}_{28}\text{H}_{30}\text{N}_4\text{O}_5$   
MW: 502.57  $\text{g} \cdot \text{mol}^{-1}$  + TFA

To a solution of **CPT-PNP** (20 mg, 40  $\mu\text{mol}$ , 1 equiv.) in dry  $\text{CH}_2\text{Cl}_2$  was added compound **5** (36 mg, 155  $\mu\text{mol}$ , 4 equiv.) under nitrogen atmosphere. The mixture was stirred at 20 °C overnight. The crude product [ $R_f$  = 0.83 (9:1  $\text{CH}_2\text{Cl}_2/\text{MeOH}$ ) mixture of diastereoisomers.] was dissolved in dry  $\text{CH}_2\text{Cl}_2$  (800  $\mu\text{L}$ , 0.05 M) and treated following General Procedure C. The crude product was then purified by HPLC (eluent A:  $\text{H}_2\text{O}$  + 0.1% TFA; eluent B: MeCN, ramp from 0% B (at min 1) to 60% B (at min 10.5),  $t_R$  (product): 9.8 min). The product was isolated as a mixture of diastereoisomers and lyophilized to give **Sp4-CPT** as a yellow solid (22 mg, 89% over two steps).

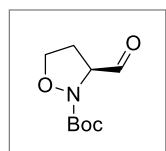
MS (ESI):  $m/z$  calcd. for  $[\text{C}_{28}\text{H}_{30}\text{N}_4\text{O}_5]^+$ : 503.23  $[M+H]^+$ , found: 503.37; HRMS (ESI)  $m/z$  calcd. for  $[\text{C}_{28}\text{H}_{30}\text{N}_4\text{O}_5]^+$ : 503.2294  $[M+H]^+$ , found: 503.2302.

### Synthesis of Sp5-CPT



**Scheme S3.** REAGENTS AND CONDITIONS: a) 1 M DIBAL-H in Hexane, dry  $\text{CH}_2\text{Cl}_2$ , -78 °C, 2h; b)  $\text{MeNH}_2$ ,  $\text{NaBH}(\text{OAc})_3$ , dry  $\text{CH}_2\text{Cl}_2$ , overnight; c) **CPT-PNP**, dry  $\text{CH}_2\text{Cl}_2$ , r.t. 3h; d) TFA/ $\text{CH}_2\text{Cl}_2$  1:2, 0 °C to r.t., 45 min.

### *Tert*-butyl (*S*)-3-formylisoxazolidine-2-carboxylate (**7**)



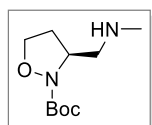
$\text{C}_9\text{H}_{15}\text{NO}_4$   
MW: 201.22  $\text{g} \cdot \text{mol}^{-1}$

Ethyl ester **6**<sup>5</sup> (150 mg, 611  $\mu\text{mol}$ , 1 equiv.) was dissolved in  $\text{CH}_2\text{Cl}_2$  (0.2 M) and treated following General Procedure A. Crude product was purified by column chromatography ( $\text{CH}_2\text{Cl}_2/\text{MeOH}$ , MeOH gradient from 2% to 5%). Final aldehyde **7** was obtained as a colourless oil (56 mg, 46%).

$R_f$  = 0.35 (1:1 EtOAc/Hex, stained with ninhydrin);  $^1\text{H}$  NMR (400 MHz,  $\text{CDCl}_3$ )  $\delta$  9.61 (d,  $J$  = 1.4 Hz, 1H), 4.59 (dd,  $J$  = 9.1, 4.6 Hz, 1H), 4.07 (m, 1H), 3.78 (dd,  $J$  = 16.3, 9.1 Hz, 1H), 2.58-2.38 (m, 2H), 1.52 (s, 9H) ppm.

5 C.E. Murar, T. J. Harmand, J. W. Bode, *Bioorg. Med. Chem.* 2017, **25**, 4996.

*O*-acetyl-*N*-(((*S*)-2-(*tert*-butoxycarbonyl)isoxazolidin-3-yl)methyl)-*N*-methylhydroxylammonium (**8**)

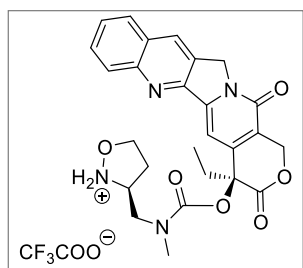


$C_{10}H_{20}N_2O_3$   
MW: 216.28 g · mol<sup>-1</sup>

Aldehyde **7** (56 mg, 278 μmol, 1 equiv.) was dissolved in a 10% mixture of AcOH in CH<sub>2</sub>Cl<sub>2</sub> (556 μL in 5.56 mL CH<sub>2</sub>Cl<sub>2</sub>) under nitrogen atmosphere and treated with methylamine (33% wt in absolute ethanol, 138 μL, 1.11 mmol, 4 equiv.) and a reducing agent following General Procedure B. The crude product was purified with column chromatography (gradient from 10 to 20% MeOH in CH<sub>2</sub>Cl<sub>2</sub>), to give amine **8** (22 mg, 30%) as an oil.

$R_f$  = 0.38 (15% MeOH in CH<sub>2</sub>Cl<sub>2</sub> + 0.2% TEA, stained with ninhydrin); <sup>1</sup>H NMR (400 MHz, MeOD) δ 4.53 (m, 1H), 4.12 (m, 1H), 3.69 (m, 1H), 3.10 (dd,  $J$  = 12.9, 3.7 Hz, 1H), 2.99 (dd,  $J$  = 12.9, 10.4 Hz, 1H), 2.71 (s, 3H), 2.54 (m, 1H), 1.99 (m, 1H), 1.51 (s, 9H) ppm.

### Sp5-CPT



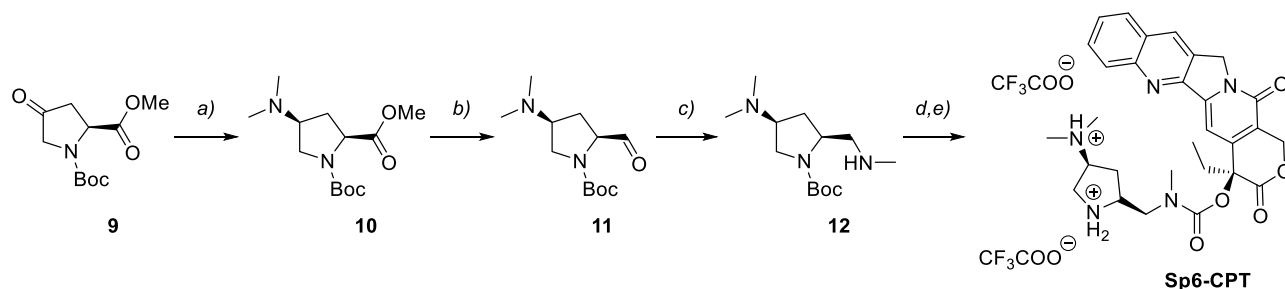
$C_{26}H_{26}N_4O_6$   
MW: 490.52 g · mol<sup>-1</sup> + TFA

To a solution of **CPT-PNP** (7 mg, 14 μmol, 1 equiv.) in dry CH<sub>2</sub>Cl<sub>2</sub> was added compound **8** (14 mg, 49 μmol, 3.5 equiv.) under nitrogen atmosphere followed by DIPEA (10 μL, 56 μmol, 4 equiv.). The reaction was stirred at 20 °C for 2 h. The crude product [ $R_f$  = 0.24 (9:1 CH<sub>2</sub>Cl<sub>2</sub>/MeOH); MS (ESI):  $m/z$  calcd. for [C<sub>31</sub>H<sub>34</sub>N<sub>4</sub>O<sub>8</sub>]<sup>+</sup>: 591.24 [ $M+H$ ]<sup>+</sup>; found: 590.20.] was dissolved in dry CH<sub>2</sub>Cl<sub>2</sub> (800 μL, 0.05 M) and treated with TFA following General Procedure C. The crude product was then purified by HPLC (eluent A: H<sub>2</sub>O + 0.1% TFA; eluent B: MeCN, ramp from 10% B (at min 1) to 57% B (at min 10),  $t_R$  (product): 9.0 min). The purified product was lyophilized to give **Sp5-CPT** as a yellow solid (20 mg, 83% over two steps).

MS (ESI):  $m/z$  calcd. for [C<sub>26</sub>H<sub>26</sub>N<sub>4</sub>O<sub>6</sub>]<sup>+</sup>: 513.17 [ $M+Na$ ]<sup>+</sup>, found: 513.20; HRMS (ESI)  $m/z$  calcd.. for [C<sub>26</sub>H<sub>26</sub>N<sub>4</sub>O<sub>6</sub>]<sup>+</sup>: 491.1931 [ $M+H$ ]<sup>+</sup>, found: 491.1933,  $m/z$  calcd. for [C<sub>26</sub>H<sub>26</sub>N<sub>4</sub>O<sub>6</sub>]<sup>+</sup>: 513.1750 [ $M+Na$ ]<sup>+</sup>, found: 513.1752.

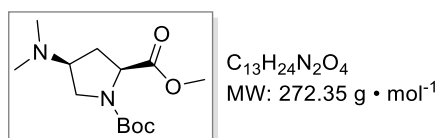


## Synthesis of Sp6-CPT



**Scheme S4.** REAGENTS AND CONDITIONS: a) HNMe<sub>2</sub>, NaBH<sub>3</sub>CN, AcOH in THF, 40 °C, 3h; b) DIBAL-H, dry CH<sub>2</sub>Cl<sub>2</sub>, -80 °C, 2h; c) MeNH<sub>2</sub>, NaBH(OAc)<sub>3</sub>, AcOH in dry CH<sub>2</sub>Cl<sub>2</sub>, r.t. 6h; d) **CPT-PNP** in dry CH<sub>2</sub>Cl<sub>2</sub>, r.t. 3h; e) TFA/CH<sub>2</sub>Cl<sub>2</sub> 1:2, 0 °C to r.t., 45 min.

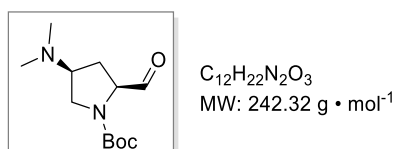
**1-(tert-butyl) 2-methyl (2S,4S)-4-(dimethylamino)pyrrolidine-1,2-dicarboxylate (10):**



To a stirred solution of ketone **9** (150 mg, 620 μmol, 1 equiv.) in dry THF (4.5 mL) dimethylamine (2.0 M in MeOH, 1.24 mL, 2.48 mmol, 4 equiv.) and acetic acid (53 μL, 930 μmol, 1.5 equiv.) were added under nitrogen atmosphere. NaBH<sub>3</sub>CN (117 mg, 1.86 mmol, 3 equiv.) was added and the mixture was stirred at r.t. for 2 h. THF was evaporated in vacuo. The crude solid was dissolved in ethyl acetate (50 mL) and transferred into a separatory funnel. A saturated aqueous sodium bicarbonate (20 mL) was added, followed by layer separation. The organic phase was then washed with brine (10 mL), dried and concentrated. The solid crude was purified with flash chromatography (gradient: from 1% to 4% MeOH in CH<sub>2</sub>Cl<sub>2</sub>) to obtain the final product as a yellow oil (156 mg, 93%).

$R_f = 0.40$  (9:1 CH<sub>2</sub>Cl<sub>2</sub>/MeOH); <sup>1</sup>H NMR (400 MHz, MeOD) δ 4.31 (m, 1H), 3.91 (dd,  $J = 10.0, 7.7$  Hz, 1H), 3.82 (m, 1H), 3.77 (bs, 3H), 3.53 (m, 1H), 2.73-2.63 (m, 7H), 2.18 (m, 1H), 1.47 (s, 9H, rotamer A), 1.41 (s, 9H, rotamer B) ppm; MS (ESI):  $m/z$  calcd. for [C<sub>13</sub>H<sub>24</sub>N<sub>2</sub>O<sub>4</sub>]<sup>+</sup>: 273.18 [ $M+H$ ]<sup>+</sup>, found: 273.12.

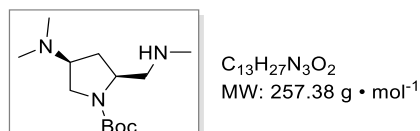
**Tert-butyl (2S,4S)-4-(dimethylamino)-2-formylpyrrolidine-1-carboxylate (11)**



Ester **10** (114 mg, 420  $\mu\text{mol}$ , 1 equiv.) was dissolved in dry  $\text{CH}_2\text{Cl}_2$  (3.5 mL, 0.12 M) and treated following General Procedure A. Crude product was purified by column chromatography (gradient: from 2% to 5% of MeOH in  $\text{CH}_2\text{Cl}_2$ ). Final aldehyde **11** was obtained as a colourless oil (58 mg, 58%).

$R_f = 0.55$  (9:1  $\text{CH}_2\text{Cl}_2/\text{MeOH}$ ); MS (ESI):  $m/z$  calcd. for  $[\text{C}_{12}\text{H}_{22}\text{N}_2\text{O}_3]^+$ : 243.17  $[M+H]^+$ , found: 243.14.

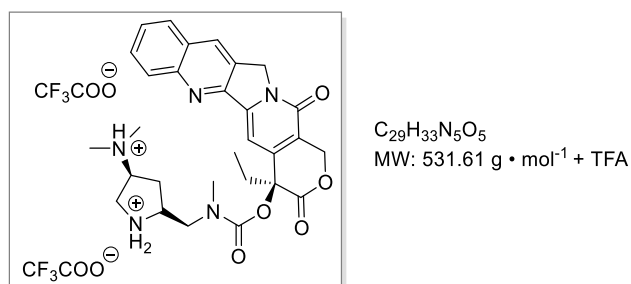
*Tert-butyl (2S,4S)-4-(dimethylamino)-2-((methylamino)methyl) pyrrolidine-1-carboxylate (12)*



Aldehyde **11** (58 mg, 240  $\mu\text{mol}$ , 1 equiv.) was dissolved in  $\text{CH}_2\text{Cl}_2/\text{AcOH}$  (5 mL + 500  $\mu\text{L}$ ) under nitrogen atmosphere and treated with methylamine (33% wt in absolute ethanol, 120  $\mu\text{L}$ , 960  $\mu\text{mol}$ , 4 equiv.) following General Procedure B. The crude product was then purified by HPLC (eluent A:  $\text{H}_2\text{O}$  + 0.1% AcOH; eluent B: MeCN, ramp from 10% B (at min 1) to 38% B (at min 12),  $t_R$  (product): 5.6 min). The purified product was lyophilized to give amine **12** as a yellow solid (53 mg, 86% over two steps).

MS (ESI):  $m/z$  calcd. for  $[\text{C}_{13}\text{H}_{27}\text{N}_3\text{O}_2]^+$ : 258.22  $[M+H]^+$ , found: 258.18.

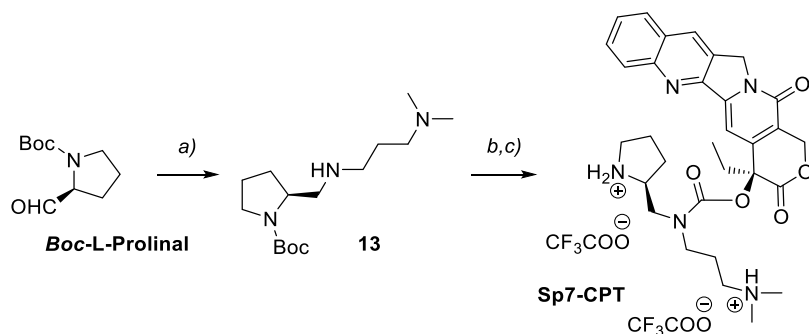
### Sp6-CPT



To a solution of **CPT-PNP** (6 mg, 13  $\mu\text{mol}$ , 1 equiv.) in dry  $\text{CH}_2\text{Cl}_2$  was added compound **12** (10 mg, 39  $\mu\text{mol}$ , 3 equiv.) under nitrogen atmosphere followed by DIPEA (9  $\mu\text{L}$ , 52  $\mu\text{mol}$ , 4 equiv.). The reaction was stirred at 20  $^\circ\text{C}$  for 2h. The crude product [ $R_f = 0.40$  (9:1  $\text{CH}_2\text{Cl}_2/\text{MeOH}$ )] was dissolved in dry  $\text{CH}_2\text{Cl}_2$  (800  $\mu\text{L}$ , 0.05 M) and treated following General Procedure C. The crude product was then purified by HPLC (eluent A:  $\text{H}_2\text{O}$  + 0.1% TFA; eluent B: MeCN, ramp from 0% B (at min 1) to 60% B (at min 10.5),  $t_R$  (product): 8.9 min). The pure fractions lyophilized to give carbamate **Sp6-CPT** as a yellow solid (21 mg, 96% over two steps).

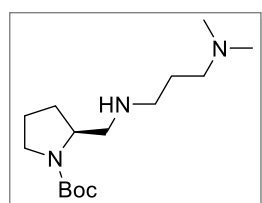
MS (ESI):  $m/z$  calcd. for  $[C_{29}H_{33}N_5O_5]^+$ : 532.26  $[M+H]^+$ , found: 532.45; HRMS (ESI)  $m/z$  calcd. for  $[C_{29}H_{33}N_5O_5]^+$ : 532.2560  $[M+H]^+$ , found: 532.2563,  $m/z$  calcd. for  $[C_{29}H_{33}N_5O_5]^+$ : 554.2379  $[M+Na]^+$ , found: 554.2380.

## Synthesis of Sp7-CPT



**Scheme S5.** REAGENTS AND CONDITIONS: a) *N,N*-dimethyl-1,3-propanediamine, NaBH(OAc)<sub>3</sub>, AcOH in dry CH<sub>2</sub>Cl<sub>2</sub>, r.t., overnight; b) CPT-PNP in dry CH<sub>2</sub>Cl<sub>2</sub>, r.t. 3h; c) TFA/ CH<sub>2</sub>Cl<sub>2</sub> 1:2, 0 °C to r.t., 45 min.

### Tert-butyl 2-(((3-(dimethylamino)propyl)amino)methyl)pyrrolidine-1-carboxylate (**13**)

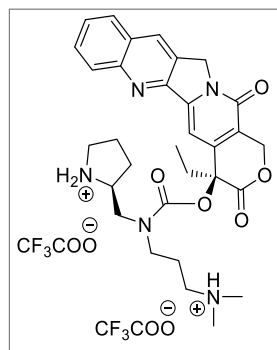


C<sub>15</sub>H<sub>31</sub>N<sub>3</sub>O<sub>2</sub>  
MW: 285.43 g • mol<sup>-1</sup>

Boc-(L)-Proline (187 μL, 1 mmol, 1 equiv.) was dissolved in a 10% AcOH solution in CH<sub>2</sub>Cl<sub>2</sub> (20 mL + 2 mL AcOH) under nitrogen atmosphere and treated following General Procedure B with *N,N*-dimethyl-1,3-propanediamine (500 μL, 4 mmol, 4 equiv.). The product was obtained as a colourless oil (260 mg, 91%).

<sup>1</sup>H NMR (400 MHz, MeOD) δ 3.89 (bs, 1H), 3.36 (m, 1H), 2.79 (dd, *J* = 11.7, 4.9 Hz, 1H), 2.67-2.60 (m, 2H), 2.55 (dd, *J* = 7.6, 11.7 Hz, 1H), 2.39-2.34 (m, 2H), 2.25 (s, 6H), 2.02-1.79 (m, 5H), 1.74-1.66 (m, 2H), 1.47 (s, 9H) ppm.

### *N,N*-dimethylpropanediamine-CPT module (**Sp7-CPT**)



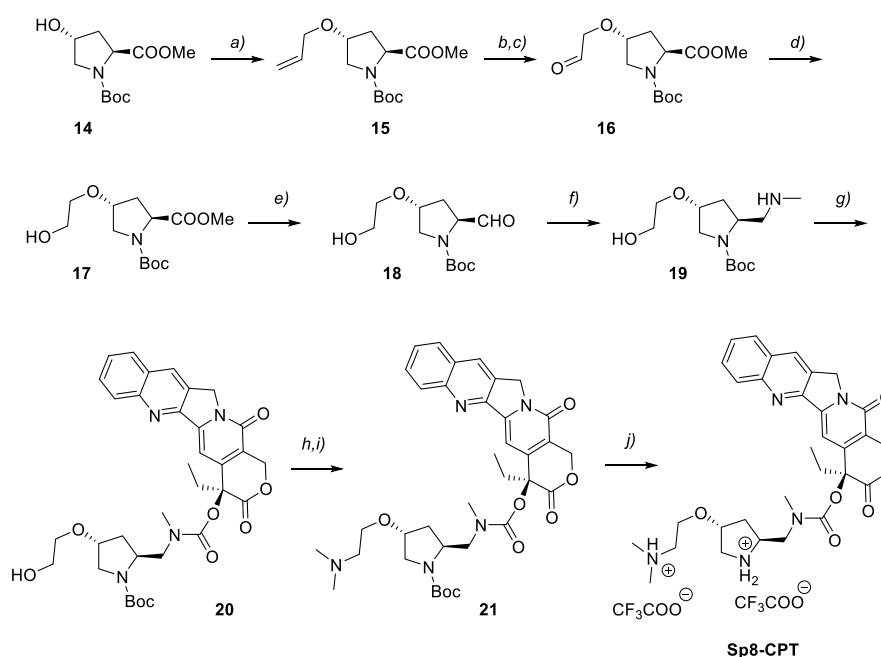
C<sub>31</sub>H<sub>37</sub>N<sub>5</sub>O<sub>5</sub>  
MW: 559.67 g • mol<sup>-1</sup> + TFA

To a solution of CPT-PNP (7 mg, 14 μmol, 1 equiv.) in dry CH<sub>2</sub>Cl<sub>2</sub> was added amine **13** (12 mg, 41 μmol, 3 equiv.) under nitrogen atmosphere followed by DIPEA (10 μL, 56 μmol, 4 equiv.). The reaction was

stirred at 20 °C for 2h. The crude product [ $R_f = 0.24$  (9:1 CH<sub>2</sub>Cl<sub>2</sub>/MeOH); MS (ESI):  $m/z$  calcd. for [C<sub>36</sub>H<sub>45</sub>N<sub>5</sub>O<sub>7</sub>]<sup>+</sup>: 660.34 [M+H]<sup>+</sup>, found: 660.32;  $m/z$  calcd. for [C<sub>36</sub>H<sub>45</sub>N<sub>5</sub>O<sub>7</sub>]<sup>+</sup>: 682.32 [M+Na]<sup>+</sup>, found: 682.33.] was dissolved in dry CH<sub>2</sub>Cl<sub>2</sub> (800 μL, 0.05 M) and treated following General Procedure C. The crude product was then purified by HPLC [eluent A: H<sub>2</sub>O + 0.1% TFA; eluent B: MeCN, ramp from 10% B (at min 1) to 60% B (at min 10.5),  $t_R$  (product): 8.6 min]. The purified product was lyophilized to give **Sp7-CPT** as a yellow solid (20 mg, 90% over two steps).

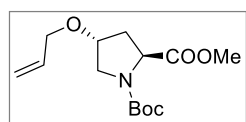
MS (ESI):  $m/z$  calcd. for [C<sub>31</sub>H<sub>37</sub>N<sub>5</sub>O<sub>5</sub>]<sup>+</sup>: 560.29 [M+H]<sup>+</sup>, found: 560.41; HRMS (ESI)  $m/z$  calcd. for [C<sub>31</sub>H<sub>37</sub>N<sub>5</sub>O<sub>5</sub>]<sup>+</sup>: 560.2873 [M+H]<sup>+</sup>, found: 560.2870.

## Synthesis of Sp8-CPT



**Scheme S6.** REAGENTS AND CONDITIONS: a) allyl bromide, KHMDS, THF, 0 °C to r.t., overnight; b) OsO<sub>4</sub> (2% mol), NMO·H<sub>2</sub>O, THF/H<sub>2</sub>O (2:1), 0 °C to r.t., overnight; c) NaIO<sub>4</sub>, THF/H<sub>2</sub>O (2:1), r.t., 1h; d) NaBH<sub>4</sub>, MeOH, 0 °C to r.t., 2.5h; e) DIBAL-H, CH<sub>2</sub>Cl<sub>2</sub>, -78 °C, 1.5h; f) MeNH<sub>2</sub>, NaBH(OAc)<sub>3</sub>, CH<sub>2</sub>Cl<sub>2</sub>, AcOH, r.t., 60h; g) **CPT-PNP**, DIPEA, CH<sub>2</sub>Cl<sub>2</sub>, r.t., 3h; h) **DMP**, CH<sub>2</sub>Cl<sub>2</sub>, 0 °C to r.t., 1 h; i) MeNH<sub>2</sub>, NaBH(OAc)<sub>3</sub>, CH<sub>2</sub>Cl<sub>2</sub>, AcOH, r.t., overnight; j) TFA/ CH<sub>2</sub>Cl<sub>2</sub> 1:2, 0 °C to r.t., 1h.

### Boc-Hyp(AlI)-OMe (15)



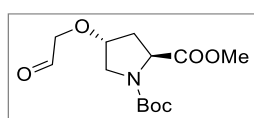
C<sub>14</sub>H<sub>23</sub>NO<sub>5</sub>  
MW: 285.34 g · mol<sup>-1</sup>

To a stirred solution of Boc-Hyp(AlI)-OMe **14**<sup>3</sup> (491 mg, 2.00 mmol, 1 equiv.) in dry THF (8 mL) cooled to 0 °C under nitrogen atmosphere was added a 0.5 M solution of KHMDS in toluene (4.8 mL, 2.40 mmol, 1.2 equiv.). The mixture was stirred for 5 min at 0 °C, then allyl bromide (208 μL, 2.40 mmol, 1.2 equiv.) was added at 0 °C. The reaction mixture was stirred overnight at r.t. and then water (5 mL) was added

and THF was evaporated in vacuo. The aqueous layer was extracted with CH<sub>2</sub>Cl<sub>2</sub> (3 x 30 mL). The combined organic layer was dried, and concentrated. The crude product was purified through flash chromatography (8:2, Hex/AcOEt), to give ether **15** as a colorless oil (374 mg, 65%).

$R_f = 0.34$  (8:2, Hex/AcOEt stained with ceric ammonium molybdate solution); <sup>1</sup>H NMR (400 MHz, CDCl<sub>3</sub>)  $\delta$  5.86 (m, 1H), 5.30-5.14 (m, 2H), 4.37 (m, 1H), 4.10 (m, 1H), 4.02-3.91 (m, 2H), 3.72 (s, 3H, rotamer A), 3.71 (s, 3H, rotamer B), 3.68-3.45 (m, 2H), 2.39-2.03 (m, 2H), 1.47-1.40 (m, 9H) ppm; MS (ESI):  $m/z$  calcd. for [C<sub>14</sub>H<sub>23</sub>NO<sub>5</sub>]<sup>+</sup>: 308.15 [M+Na]<sup>+</sup>, found: 308.07.

### Boc-Hyp(2-oxoethoxy)-OMe (**16**)

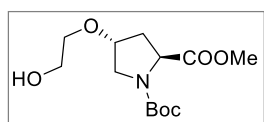


C<sub>13</sub>H<sub>21</sub>NO<sub>6</sub>  
MW: 287.31 g • mol<sup>-1</sup>

To an ice-cold solution of terminal alkene **15** (200 mg, 700  $\mu$ mol, 1 equiv.) and 4-methylmorpholine *N*-oxide monohydrate (194 mg, 1.44 mmol, 2 equiv.) in a 2:1 THF/H<sub>2</sub>O mixture (4.5 mL), OsO<sub>4</sub> (2.5 wt% solution in *t*-BuOH, 176  $\mu$ L, 14  $\mu$ mol, 0.02 equiv.) was added. The mixture was stirred for 3 h at 0 °C and then allowed to warm to r.t. and stirred overnight. Solid sodium hydrogen sulfite was added and the mixture as stirred for 1 h at r.t. The mixture was filtered through a pad of silica and rinsed with THF. Volatiles removal led to the crude 1,2-diol intermediate as a yellow oil (288 mg), which was used in the following step without purification. The diol was dissolved in a 2:1 THF/H<sub>2</sub>O solution (6.9 mL) and sodium periodate (305 mg, 1.43 mmol, 2 equiv.) was added. The mixture was stirred at r.t. for 1 h. Water (4 mL) was added and THF was evaporated in vacuo. The aqueous layer was extracted with CH<sub>2</sub>Cl<sub>2</sub> (3 x 30 mL). The combined organic layers were dried, filtered and concentrated in vacuo, to give aldehyde **16** as a yellow oil (207 mg, quant), which was rapidly used in the following step.

$R_f = 0.36$  (8:2, AcOEt/Hex stained with ceric ammonium molybdate solution).

### Boc-Hyp(2-hydroxyethoxy)-OMe (**17**)



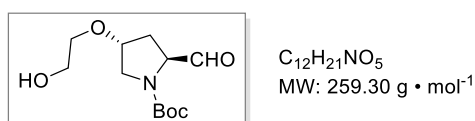
C<sub>13</sub>H<sub>23</sub>NO<sub>6</sub>  
MW: 289.33 g • mol<sup>-1</sup>

Aldehyde **16** (206 mg, 0.72 mmol, 1 equiv.) was dissolved in dry MeOH (7.2 mL) under nitrogen atmosphere and cooled to 0 °C. NaBH<sub>4</sub> (41 mg, 1.08 mmol, 1.5 equiv.) was added at 0 °C and then the reaction mixture was allowed to warm to r.t. The reaction mixture was stirred at r.t. for 2.5 h. After concentrating the solvent, 5 mL of a sat. aq. NaHCO<sub>3</sub> solution were added and the aqueous layer was

then extracted with  $\text{CH}_2\text{Cl}_2$  (3 x 30 mL). The combined organic layers were dried ( $\text{Na}_2\text{SO}_4$ ), filtered and concentrated in vacuo. The crude product was purified through flash column chromatography (3% of MeOH in  $\text{CH}_2\text{Cl}_2$ ), to give alcohol **17** as a colorless oil (176 mg, 85%).

$R_f = 0.40$  (95:5,  $\text{CH}_2\text{Cl}_2/\text{MeOH}$  stained with  $\text{KMnO}_4$  and conc.  $\text{H}_2\text{SO}_4$ );  $^1\text{H NMR}$  (400 MHz,  $\text{CDCl}_3$ )  $\delta$  4.39 (m, 1H), 4.17-4.06 (m, 2H), 3.74-3.70 (m, 4H), 3.69-3.45 (m, 5H), 2.47-2.03 (m, 2H), 1.47-1.41 (m, 9H) ppm; MS (ESI):  $m/z$  calcd. for  $[\text{C}_{13}\text{H}_{23}\text{NO}_6]^+$ : 312.14  $[\text{M}+\text{Na}]^+$ , found: 312.19.

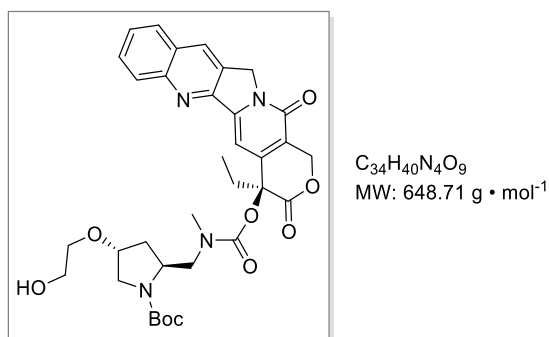
### *Boc-Hyp(2-hydroxyethoxy)-CHO (18)*



A solution of methylester **17** (109 mg, 380  $\mu\text{mol}$ , 1 equiv.) in dry  $\text{CH}_2\text{Cl}_2$  (3.8 mL) and a solution of DIBAL-H (1 M in toluene, 1 mL) under nitrogen atmosphere were separately cooled to  $-78^\circ\text{C}$  in an acetone/dry-ice bath. Portions of the cold DIBAL-H solution (10 x 80  $\mu\text{L}$ , 790  $\mu\text{mol}$ , 2.1 equiv.) were rapidly transferred to the stirring **17** solution. The mixture was then stirred at  $-78^\circ\text{C}$  for 1.5 h, followed by addition of  $\text{CH}_2\text{Cl}_2$  (30 mL) at  $-78^\circ\text{C}$ . The mixture was then warmed to  $0^\circ\text{C}$  (ice-water bath), followed by sequential addition of water (32  $\mu\text{L}$ ), 15% aq. NaOH (32  $\mu\text{L}$ ) and again water (79  $\mu\text{L}$ ). The resulting emulsion was warmed to r.t. and stirred for 15 min. After the addition of  $\text{Na}_2\text{SO}_4$ , the mixture was stirred for additional 15 min. The mixture was then filtered and concentrated, to give aldehyde **18** as a yellow oil (86 mg, 88%), which was immediately used in the following step, without purification.

$R_f = 0.43$  (95:5,  $\text{CH}_2\text{Cl}_2/\text{MeOH}$  stained with 2,4-dinitrophenylhydrazine).

### *Boc-Hyp(2-hydroxyethoxy)-CPT (20)*

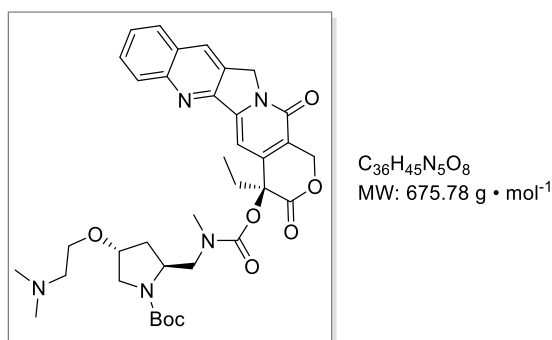


Aldehyde **18** (86 mg, 330  $\mu\text{mol}$ , 1 equiv.) was dissolved in  $\text{CH}_2\text{Cl}_2$  (6.5 mL) containing AcOH (28  $\mu\text{L}$ , 1.5 equiv.) under nitrogen atmosphere and treated with methylamine (33% wt in absolute ethanol, 165  $\mu\text{L}$ ,

1.33 mmol, 4 equiv.) following General Procedure B. The crude product was purified with flash chromatography (10% MeOH in CH<sub>2</sub>Cl<sub>2</sub> + 1% TEA) to obtain secondary amine **19** (49 mg, 200 μmol). The latter was dissolved in dry CH<sub>2</sub>Cl<sub>2</sub> (4 mL), followed by addition of **CPT-PNP** (122 mg, 240 μmol, 1.2 equiv.) and DIPEA (138 μL, 800 μmol, 4 equiv.). The mixture was stirred at r.t. for 3 h. After solvent removal, the crude product (200 mg) was purified through flash chromatography (gradient: from 1% to 10% MeOH in CH<sub>2</sub>Cl<sub>2</sub>), to give carbamate **20** as a yellow solid (107 mg, 84%).

MS (ESI): *m/z* calcd. for [C<sub>34</sub>H<sub>40</sub>N<sub>4</sub>O<sub>9</sub>]<sup>+</sup>: 671.27 [*M*+Na]<sup>+</sup>, found: 671.52.

### *Boc-Sp8-CPT (21)*

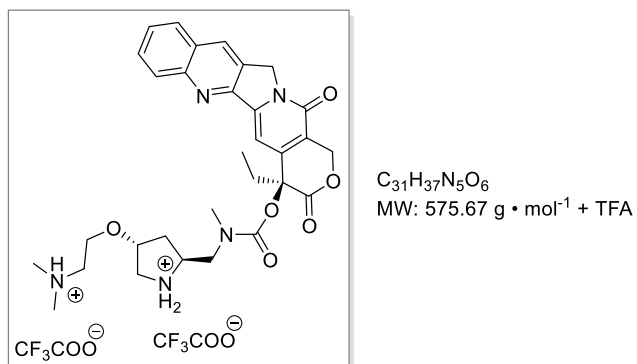


Alcohol **20** (19 mg, 29 μmol, 1 equiv.) was dissolved in dry CH<sub>2</sub>Cl<sub>2</sub> (3 mL) under nitrogen atmosphere and cooled to 0 °C. After the addition of a 0.3 M DMP solution in CH<sub>2</sub>Cl<sub>2</sub> (308 μL, 92 μmol, 3 equiv.) at 0 °C, the mixture was warmed to r.t. and stirred for 1 h. After the addition of MeOH (200 μL) at 0 °C and removal of the solvent, the residue was dissolved in a 10% MeOH solution in CH<sub>2</sub>Cl<sub>2</sub> and filtered over a pad of silica (rinsed with 10% MeOH solution in CH<sub>2</sub>Cl<sub>2</sub>). The crude product was dissolved in CH<sub>2</sub>Cl<sub>2</sub> (1 mL) under nitrogen atmosphere and treated with AcOH (4 μL, 1.5 equiv.) and dimethylamine (2 M in THF, 97 μL, 190 μmol, 4 equiv.) following General Procedure B. The crude product was filtered over a pad of silica and eluted with a 9:1 CH<sub>2</sub>Cl<sub>2</sub>/MeOH mixture (50 mL) and later with a 9:1 CH<sub>2</sub>Cl<sub>2</sub>/MeOH mixture + 1% TEA (50 mL). After solvent removal, the crude mixture was purified by HPLC (eluent A: H<sub>2</sub>O + 0.1% AcOH, eluent B: MeCN, ramp from 15% B at min 0.5 to 70% B at min 9, *t<sub>R</sub>* (product): 6.5 min). The pure fractions were lyophilized to give **21** as a yellow solid (14 mg, 65% over two steps).

MS (ESI): *m/z* calcd. for [C<sub>36</sub>H<sub>46</sub>N<sub>5</sub>O<sub>8</sub>]<sup>+</sup>: 676.33 [*M*+H]<sup>+</sup>, found: 676.39.



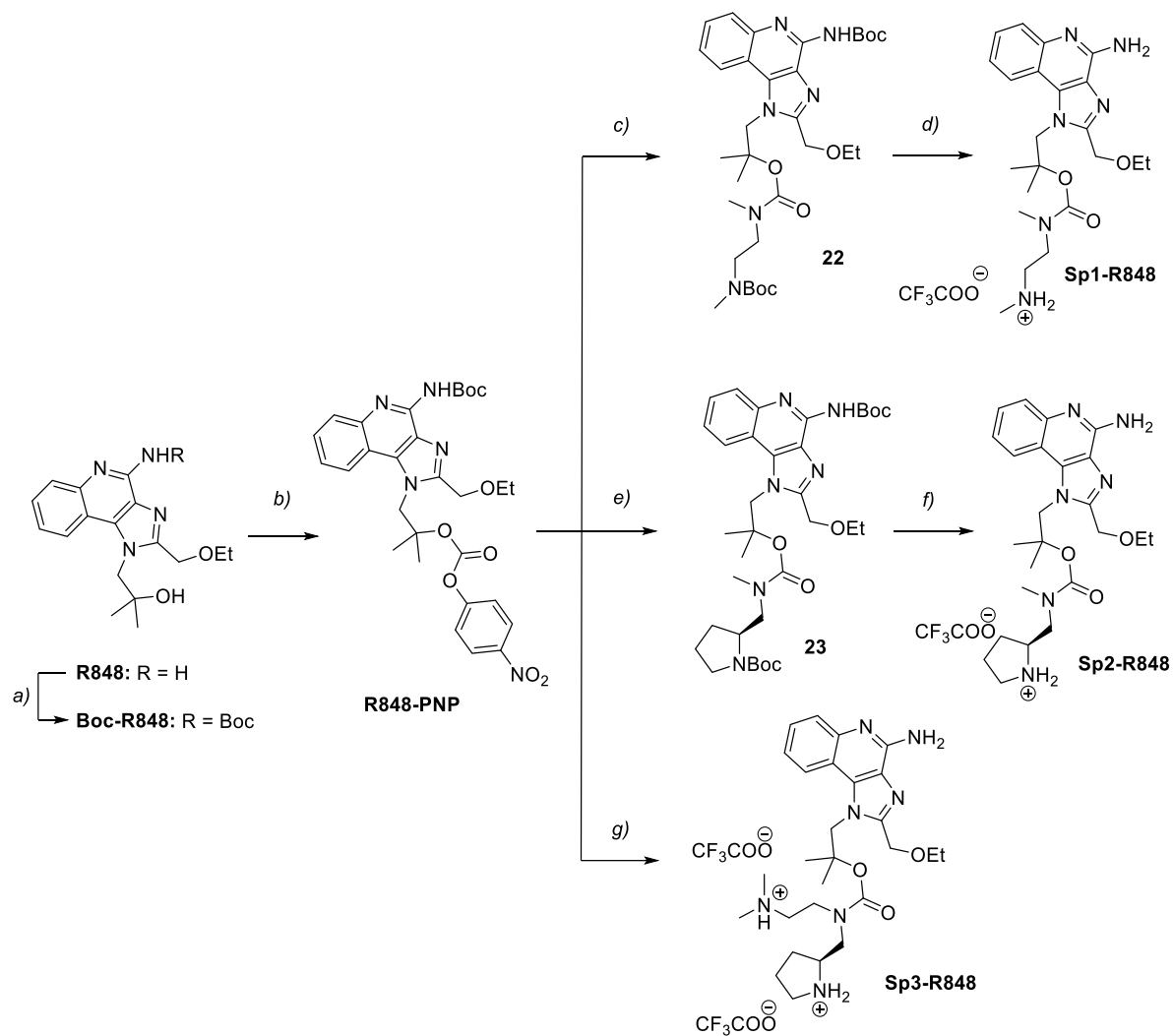
## Sp8-CPT



**21** (5 mg, 7 μmol, 1 equiv.) was dissolved in dry CH<sub>2</sub>Cl<sub>2</sub> (250 μL, 0.03 M) and treated with TFA following General Procedure C. The crude product was then purified by HPLC (eluent A: H<sub>2</sub>O + 0.1% TFA, eluent B: MeCN, ramp from 15% B at min 1 to 60% B at min 10.5, *t<sub>R</sub>* (product): 7.2 min). The pure fractions were lyophilized to give carbamate **Sp8-CPT** as a yellow solid (4 mg, 71%).

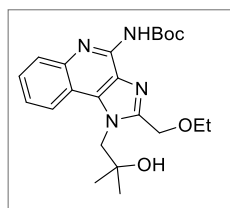
HRMS (ESI): *m/z* calcd. for [C<sub>31</sub>H<sub>38</sub>N<sub>5</sub>O<sub>6</sub>]<sup>+</sup>: 576.2817 [M+H]<sup>+</sup>, found: 576.2831.

## Synthesis of Sp1-R848, Sp2-R848, Sp3-R848



**Scheme S7.** REAGENTS AND CONDITIONS: a)  $\text{Boc}_2\text{O}$ , TEA, THF, 0 °C to r.t. 72 h; c)  $(N\text{-Boc})\text{-}N,N'$ -dimethylethylenediamine, DIPEA,  $\text{CH}_2\text{Cl}_2$ , r.t. 2.5 h; d) TFA/  $\text{CH}_2\text{Cl}_2$ , r.t. 1 h; e) Boc-Pro-NHMe, DIPEA,  $\text{CH}_2\text{Cl}_2$ , r.t. 1h 45'; f) TFA/  $\text{CH}_2\text{Cl}_2$ , r.t. 1 h; g) **3**, DIPEA,  $\text{CH}_2\text{Cl}_2$ , r.t. 1h 45'; [2] TFA/  $\text{CH}_2\text{Cl}_2$ , r.t. 1 h.

## Boc-R848

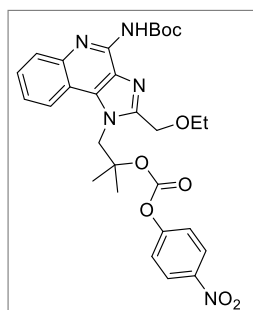


$C_{22}H_{30}N_4O_4$   
MW: 414.51 g · mol<sup>-1</sup>

**R848** (Fluorochem, 83 mg, 260 μmol, 1 equiv.) was dissolved in THF (3 ml). Boc<sub>2</sub>O (288 mg, 1.32 mmol, 5 equiv.) and TEA (183 μL, 1.32 mmol, 5 equiv.) were added at 0 °C and the reaction was stirred at r.t. for 72 h. The crude material was purified by flash chromatography (eluent 3% MeOH in CH<sub>2</sub>Cl<sub>2</sub>), to give Boc-R848 as a white foam (95 mg, 88%).

$R_f$  = 0.45 (95:5 CH<sub>2</sub>Cl<sub>2</sub>/MeOH); <sup>1</sup>H NMR (400 MHz, CDCl<sub>3</sub>) δ 8.19 (d,  $J$  = 8.3 Hz, 1H), 8.12 (d,  $J$  = 8.2 Hz, 1H), 7.58 (t,  $J$  = 7.6 Hz, 1H), 7.45 (t,  $J$  = 7.5 Hz, 1H), 4.91 (bs, 2H), 4.78 (bs, 2H), 3.67 (q,  $J$  = 7.0 Hz, 2H), 3.20 (s, 1H), 1.59 (s, 9H), 1.32 (bs, 6H), 1.26 (t,  $J$  = 7.0 Hz, 3H) ppm; <sup>13</sup>C NMR (101 MHz, CDCl<sub>3</sub>) δ 150.8, 150.6, 144.8, 144.0, 135.4, 129.9, 127.5, 124.4, 119.8, 116.5, 81.4, 71.5, 66.7, 65.0, 56.5, 28.3, 27.9, 14.9 ppm.

## R848-PNP



$C_{29}H_{33}N_5O_8$   
MW: 579.61 g · mol<sup>-1</sup>

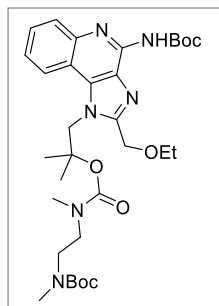
R848 *N*-Boc (30 mg, 72 μmol, 1 equiv.) was dissolved in CH<sub>2</sub>Cl<sub>2</sub> (1 mL) and cooled to 0 °C. DMAP (53 mg, 434 μmol, 6 equiv.) and 4-nitrophenyl chloroformate (44 mg, 217 μmol, 3 equiv.) were added. After 1 h, a white precipitate is observed. The mixture was stirred at r.t. for 4 h. The solution was then diluted with CH<sub>2</sub>Cl<sub>2</sub> and concentrated, and the crude product was purified through flash chromatography (eluent 6:4 AcOEt/Hex + 0.1% AcOH) affording carbonate **R848-PNP** (17 mg, 40%, residual 4-nitrophenol was detected by NMR analysis of the collected fractions).

$R_f$  = 0.78 (8:2 AcOEt:Hex 1% AcOH); <sup>1</sup>H NMR (400 MHz, CD<sub>2</sub>Cl<sub>2</sub>) δ 8.40 (d,  $J$  = 8.0 Hz, 1H), 8.21 (d,  $J$  = 8.3 Hz, 1H), 8.19 (d,  $J$  = 9.00 Hz, 2H), 8.10 (d, 4-nitrophenol), 7.78-7.66 (m, 2H), 7.13 (d,  $J$  = 9.00 Hz, 2H), 6.92 (d, 4-nitrophenol), 5.00 (bs, 2H), 4.87 (bs, 2H), 3.64 (q,  $J$  = 7.00 Hz, 2H), 2.06 (s, AcOH), 1.38

## SUPPORTING INFORMATION

(s, 9H), 1.33 (bs, 6H), 1.22 (t,  $J = 7.00$  Hz, 3H) ppm; MS (ESI)  $m/z$  calcd. for  $[C_{29}H_{33}N_5O_8]^+$ : 580.24  $[M+H]^+$ , found: 580.44;  $m/z$  calcd. for  $[C_{29}H_{33}N_5O_8]^+$ : 602.22  $[M+Na]^+$ , found: 602.53.

### Boc-Sp1-R848 (**22**)

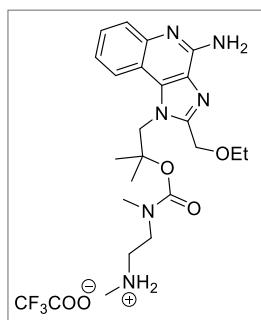


$C_{32}H_{48}N_6O_7$   
MW: 628.77  $g \cdot mol^{-1}$

Carbonate **R848-PNP** (8 mg, 14.3  $\mu$ mol, 1 equiv.) was dissolved in  $CH_2Cl_2$  (1.0 ml) and (*N*-Boc)-*N,N'*-dimethylethylenediamine<sup>4</sup> (12 mg, 63  $\mu$ mol, 4.4 equiv.) and DIPEA (5.5  $\mu$ L, 31.5  $\mu$ mol, 2.2 equiv.) were added. The reaction was stirred at r.t. for 2.5 h and the crude material was purified by flash chromatography (7:3 AcOEt:Hex + 0.1% AcOH), to give carbamate **22** as a yellow oil (6 mg, 68%).

$R_f = 0.27$  (7:3 AcOEt:Hex 1% AcOH); MS (ESI)  $m/z$  calcd. for  $[C_{32}H_{48}N_6O_7]^+$ : 629.37  $[M+H]^+$ , found: 629.15;  $m/z$  calcd. for  $[C_{32}H_{48}N_6O_7]^+$ : 651.35  $[M+Na]^+$ , found: 651.25.

### Sp1-R848

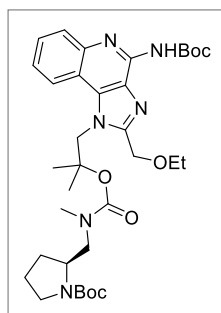


$C_{22}H_{32}N_6O_3$   
MW: 428.54  $g \cdot mol^{-1}$  + TFA

Carbamate **22** (6 mg, 9.7  $\mu$ mol, 1 equiv.) was dissolved in  $CH_2Cl_2$  (324  $\mu$ L) and treated with TFA following General Procedure C. After solvent removal, the crude material was purified by HPLC [eluent A:  $H_2O$  + 0.1% TFA; eluent B: MeCN, ramp from 10% B (at min 1) to 60% B (at min 10),  $t_R$  (product): 6.9 min]. The pure product was then lyophilized to give **Sp1-R848** as a colorless solid (3 mg, 83%).

MS (ESI)  $m/z$  calcd. for  $[C_{22}H_{32}N_6O_3]^+$ : 429.26  $[M+H]^+$ , found: 429.35; HRMS (ESI)  $m/z$  calcd. for  $[C_{22}H_{32}N_6O_3]^+$ : 429.2614  $[M+H]^+$ , found: 429.2615.

### Boc-Sp2-R848 (**23**)

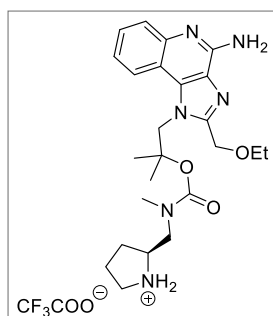


$C_{34}H_{50}N_6O_7$   
MW: 654.81 g · mol<sup>-1</sup>

Carbonate **R848-PNP** (14 mg, 24.2 μmol, 1 equiv.) was dissolved in CH<sub>2</sub>Cl<sub>2</sub> (1.7 ml). Secondary amine Boc-Pro-NHMe<sup>4</sup> (23 mg, 105.8 μmol, 4.4 equiv.) and DIPEA (9.3 μL, 96.6 μmol, 2.2 equiv.) were added and the mixture was stirred at r.t. for 1.5 h. Solvent was removed and the crude material was purified by flash chromatography (eluent 1% MeOH in CH<sub>2</sub>Cl<sub>2</sub>), to give carbamate **23** (19 mg, quant).

$R_f = 0.72$  (9:1 AcOEt:Hex); MS (ESI)  $m/z$  calcd. for [C<sub>34</sub>H<sub>50</sub>N<sub>6</sub>O<sub>7</sub>]<sup>+</sup>: 655.38 [M+H]<sup>+</sup>, found: 655.37;  $m/z$  calcd. for [C<sub>34</sub>H<sub>50</sub>N<sub>6</sub>O<sub>7</sub>]<sup>+</sup>: 677.36 [M+Na]<sup>+</sup>, found: 677.39.

### Sp2-R848

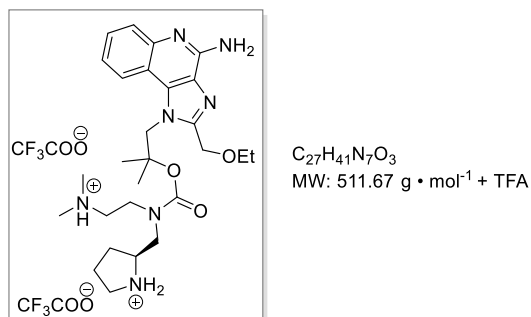


$C_{24}H_{34}N_6O_3$   
MW: 454.58 g · mol<sup>-1</sup> + TFA

Carbamate **23** (16 mg, 24.2 μmol, 1 equiv.) was dissolved in CH<sub>2</sub>Cl<sub>2</sub> (783 μL) and treated following General Procedure C. After solvent removal, the crude material was purified by HPLC [eluent A: H<sub>2</sub>O + 0.1% TFA; eluent B: MeCN, ramp from 10% B (at min 1) to 60% B (at min 10),  $t_R$  (product): 7 min]. The pure product was then lyophilized to give **Sp2-R848** as a colorless solid (18 mg, quant.).

MS (ESI)  $m/z$  calcd. for [C<sub>24</sub>H<sub>34</sub>N<sub>6</sub>O<sub>3</sub>]<sup>+</sup>: 455.28 [M+H]<sup>+</sup>, found: 455.29; HRMS (ESI)  $m/z$  calcd. for [C<sub>24</sub>H<sub>35</sub>N<sub>6</sub>O<sub>3</sub>]<sup>+</sup>: 455.2771 [M+H]<sup>+</sup>, found: 455.2776.

## Sp3-R848



Carbonate **R848-PNP** (8 mg, 14 μmol, 1 equiv.) was dissolved in CH<sub>2</sub>Cl<sub>2</sub> (1 ml), cooled to 0 °C. Amine **3** (5 mg, 42 μmol, 3 equiv.) and DIPEA (7 μL, 42 μmol, 3 equiv.) were added. The reaction was stirred at rt for 24 h. The crude material was purified by flash chromatography (eluent 5% MeOH in CH<sub>2</sub>Cl<sub>2</sub>) and the resulting carbamate was dissolved in CH<sub>2</sub>Cl<sub>2</sub> (200 μL) and treated with TFA following General Procedure C. After solvent removal, the crude material was purified by HPLC [eluent A: H<sub>2</sub>O + 0.1% TFA; eluent B: MeCN, ramp from 10% B (at min 1) to 50% B (at min 9), *t<sub>R</sub>* (product): 8.2 min]. The pure product was then lyophilized to give **Sp3-R848** as a white solid (3 mg, 31%).

HRMS (ESI) *m/z* calcd. for [C<sub>27</sub>H<sub>41</sub>N<sub>7</sub>O<sub>3</sub>]<sup>+</sup>: 512.3349 [M+H]<sup>+</sup>, found: 512.3352.

## Carbamate Cleavage Studies

### Experimental Procedure for Sp-CPT Modules

Stock solutions of lyophilized SI spacer-CPT modules (concentration: 10 mM in DMSO) were diluted 1:10 (final concentration: 1 mM) with 25 mM phosphate buffer (pH 7.4). Immediately after preparation, the mixtures were incubated at 37 °C. Aliquots were collected at different time points and diluted 1:4 (final concentration: 250 µM) with a blocking buffer (8:2 H<sub>2</sub>O/CH<sub>3</sub>CN + 0.2% TFA).

The diluted aliquots were injected into an analytical HPLC-PDA system (see Materials and Methods), using the following parameters:

Eluent A	H <sub>2</sub> O + 0.1% TFA
Eluent B	CH <sub>3</sub> CN + 0.1% TFA
Flow Rate	1 mL/min
Gradient	From 10% B to 50% B in 26 min.
UV analysis	254 nm

Areas under the curve (AUC) of the detected peaks were measured using software associated to the HPLC systems. The rate of free OH release from the starting carbamate were obtained by calculating the relative ratios of AUC values corresponding to the amine-bearing prodrug and the free payload. Data were plotted versus time and half-lives ( $t_{1/2}$ ) were calculated by non-linear fitting (exponential, one-phase decay) using GraphPad Prism software.

## Experimental Procedure for Sp-R848 modules

Stock solutions of lyophilized SI spacer-R848 modules were diluted with further DMSO and 25 mM phosphate buffer (pH 7.4) according to the following scheme:

	<b>Sp1-R848</b>	<b>Sp2-R848</b>	<b>Sp3-R848</b>
Stock solution concentration in DMSO	20 mM	100 mM	10 mM
Sample (in DMSO) (Volume % Total)	5% - [1 mM] final	1% - [1 mM] final	10% - [1 mM] final
Neat DMSO (Volume % Total)	5%	9%	-
Aq. Buffer (Volume % Total)	90%	90%	90%

Immediately after preparation, the mixtures were incubated at 37 °C and aliquots were collected at different time points and diluted 1:5 (final concentration: 200 µM) with a blocking buffer (8:2 H<sub>2</sub>O/CH<sub>3</sub>CN + 0.2% TFA).

The diluted aliquots were injected into an analytical HPLC-PDA system, using the following parameters:

Eluent A	H <sub>2</sub> O + 0.1% TFA
Eluent B	CH <sub>3</sub> CN + 0.1% TFA
Flow Rate	1 mL/min
Gradient	From 5% B to 35% B in 26 min.
UV analysis	254 nm

Areas under the curve (AUC) of the detected peaks were measured using software associated to the HPLC systems. The rate of free OH release from the starting carbamate were obtained by calculating the relative ratios of AUC values corresponding to the amine-bearing prodrug and the free payload. Data were plotted versus time and half-lives ( $t_{1/2}$ ) were calculated by non-linear fitting (exponential, one-phase decay) using GraphPad Prism software.



## Computational Studies

All calculations were run using the Schrödinger suite of programs through the Maestro graphical interface.<sup>6</sup> The following steps were implemented to identify relevant minimum-energy conformations of the model carbamates in their main ionization state at pH 7.5 (i.e. protonated pyrrolidine in **Sp2-tBu**, protonated pyrrolidine and tertiary amine in **Sp3-tBu**).

*Molecular Mechanics calculations.* Monte Carlo/energy minimization (MC/EM) conformational searches<sup>7</sup> of carbamates **Sp2-tBu** and **Sp3-tBu** were performed within the framework of MacroModel version 11.1,<sup>8</sup> using the OPLS3 force field<sup>9</sup> and the implicit water GB/SA solvation model,<sup>10</sup> to generate starting geometries for subsequent DFT calculations. The exocyclic dihedral angles of each compound were randomly varied with the usage-directed Monte Carlo conformational search. For each search, at least 1000 starting structures for each variable torsion angle were generated and minimized until the gradient was  $<0.05 \text{ kJ}\text{Å}^{-1}\text{mol}^{-1}$  using the truncated Newton–Raphson algorithm.<sup>11</sup> Duplicate conformations and those with energy  $>5 \text{ kcalmol}^{-1}$  above the global minimum were discarded.

*DFT calculations.* Representative minimum-energy geometries obtained from the MC/EM conformational search were fully optimized with DFT calculations at the B3LYP/6-31G\* level of theory using the Jaguar version 9.1.<sup>12</sup> Default convergence criteria were employed. Calculations of vibrational frequencies were carried out to ensure that stationary points were true minima on the potential energy surface. Solution phase energies of the obtained stationary points were computed at the same level of theory by single-point energy calculations including the water PBF solvent model (Poisson-Boltzmann Solvation Model in Jaguar).<sup>12</sup> Representative DFT minimum energy structures displaying relative solution energy differences within 3 kcal/mol of the global minimum are shown in Figure S2 (the *syn* 2 conformation of **Sp3-tBu** found at 4.13 kcal/mol is included for completeness). The values of the dihedral angles that distinguish these structures are reported in Table S1.  $pK_a$  values of the protonated species were calculated on the lowest energy *anti* and *syn* structure pairs by the Jaguar  $pK_a$  prediction module.

---

6 Maestro, release 2016-1, Schrödinger, LLC, New York, NY, 2016.

7 G. Chang, W. C. Guida, W. C. Still, *J. Am. Chem. Soc.* 1989, **111**, 4379.

8 MacroModel, version 11.1, Schrödinger, LLC, New York, NY, 2016.

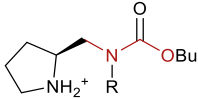
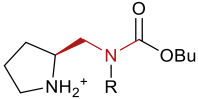
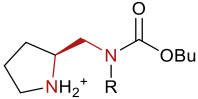
9 K. Roos, C. Wu, W. Damm, M. Reboul, J.M. Stevenson, C. Lu, M.K. Dahlgren, S. Mondal, W. Chen, L. Wang, R. Abel, R.A. Friesner, E.D. Harder, *J. Chem. Theory Comput.* 2019, **15**, 1863.

10 W. C. Still, A. Tempczyk, R. C. Hawley, T. Hendrickson, *J. Am. Chem. Soc.* 1990, **112**, 6127.

11 J. W. Ponder, F. M. Richards, *J. Comput. Chem.* 1987, **8**, 1016.

12 Jaguar, version 9.1, release 14, Schrödinger, LLC, New York, NY, 2016.

**Table S1.** Dihedral angles of the pyrrolidine-carbamate chain in representative DFT-optimized conformations of **Sp2/3-tBu**. Relative energy differences are calculated from the corresponding solution phase energies (spE).

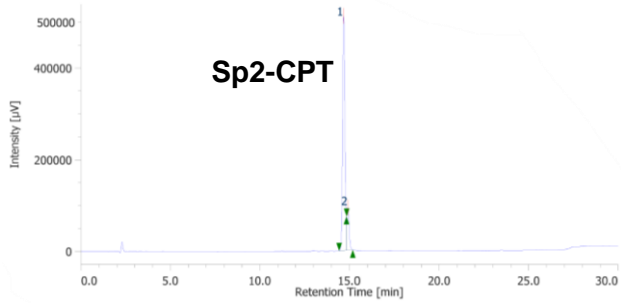
Compound	Conformation	$\Delta$ spE (kcal/mol)	Dihedral angle	Dihedral angle	Dihedral angle
			C-N-C <sub>carb</sub> -O <sub>sp</sub> <sup>3</sup> (degrees)	C-C-N-C <sub>carb</sub> (degrees)	N <sub>pyr</sub> -C-C-N <sub>carb</sub> (degrees)
					
<b>Sp2-tBu</b>	<i>anti</i> (H-bond)	0.00	-161.1°	-87.1°	67.9
	<i>anti</i> 2 (H-bond)	0.59	-161.0°	83.4°	-72.5°
	<i>syn</i> (H-bond)	2.74	19.0°	-97.9°	61.8°
	<i>anti</i> 3 (H-bond, different ring puckering)	2.88	-166.3°	-68.4°	87.1°
<b>Sp3-tBu</b>	<i>syn</i> (2 H-bonds)	0.00	15.7°	-94.0°	68.0°
	<i>anti</i> (2 H-bonds)	1.16	-164.8°	-83.6°	72.5°
	<i>anti</i> 2 (1 H-bond)	1.96	-171.5°	-79.3°	73.8°
	<i>anti</i> 3 (1 H-bond)	2.57	171.3°	73.1°	-80.8°
	<i>syn</i> 2 (1 H-bond)	4.13	9.6°	-89.7°	68.5°

## Appendix

### HPLC Data – Sp-CPT Modules

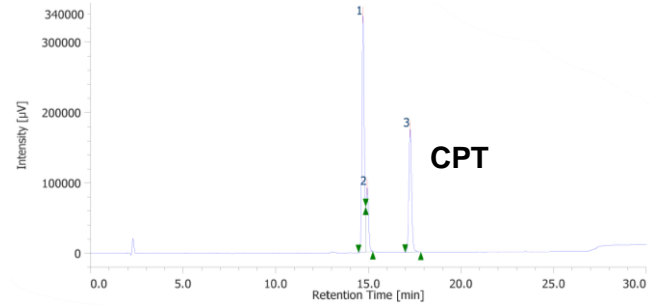
- Sp2-CPT 1 mM
- 25 mM phosphate buffer + 10 % DMSO
- pH 7.4, T: 37 °C

t = 0 h



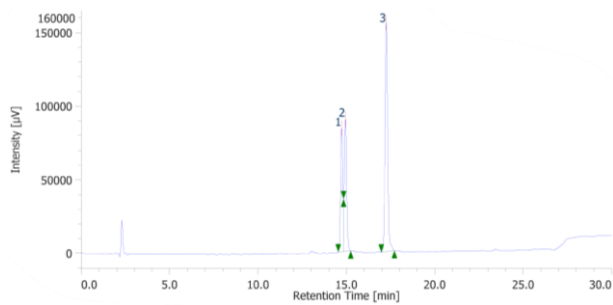
#	Peak Name	CH	tR [min]	Area [µV·sec]	Height [µV]	Area%	Height%	Resolution	Symmetry Factor	Factor
1	Unknown	9	14.7	4722012	511211	85.3	84.694	N/A	N/A	1.00000
2	Unknown	9	14.9	810993	92387	14.7	15.306	N/A	N/A	1.00000
Total				5533005	603598					

t = 1 h



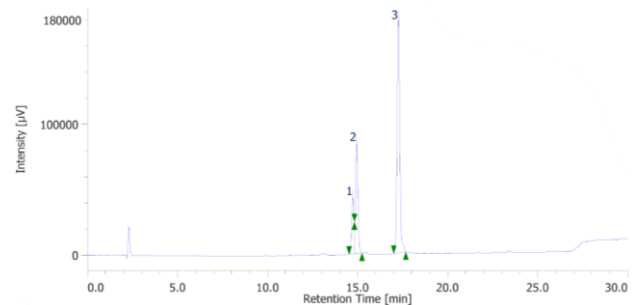
#	Peak Name	CH	tR [min]	Area [µV·sec]	Height [µV]	Area%	Height%	Resolution	Symmetry Factor	Factor
1	Unknown	9	14.7	3086164	337468	53.9	55.859	N/A	N/A	1.00000
2	Unknown	9	14.9	833652	91713	14.6	15.181	N/A	N/A	1.00000
3	Unknown	9	17.3	1804656	174966	31.5	28.961	N/A	1.047	1.00000
Total				5724472	604147					

t = 5 h



#	Peak Name	CH	tR [min]	Area [µV·sec]	Height [µV]	Area%	Height%	Resolution	Symmetry Factor	Factor
1	Unknown	9	14.7	757222	83696	23.5	25.441	0.843	N/A	1.00000
2	Unknown	9	14.9	841424	89632	26.2	27.245	8.824	N/A	1.00000
3	Unknown	9	17.3	1618228	155658	50.3	47.314	N/A	1.070	1.00000
Total				3216874	328986					

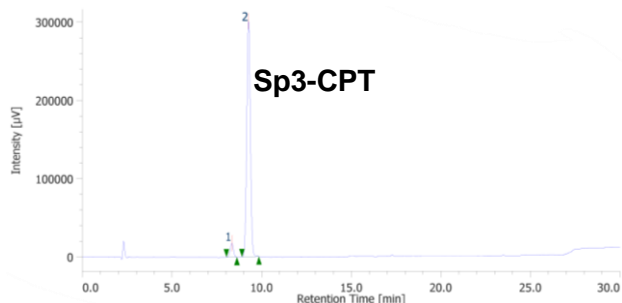
t = 8 h



#	Peak Name	CH	tR [min]	Area [µV·sec]	Height [µV]	Area%	Height%	Resolution	Symmetry Factor	Factor
1	Unknown	9	14.7	371878	43211	12.2	14.122	N/A	N/A	1.00000
2	Unknown	9	14.9	805129	84112	26.5	27.488	8.969	N/A	1.00000
3	Unknown	9	17.3	1860656	178669	61.3	58.390	N/A	1.073	1.00000
Total				3037663	305992					

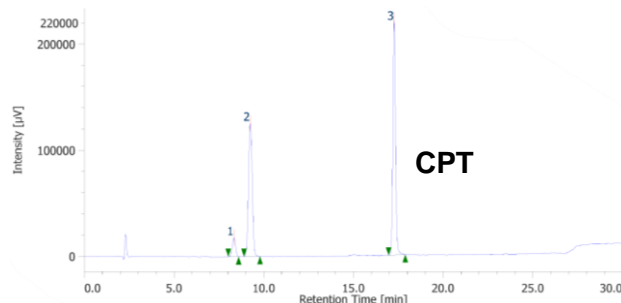
- Sp3-CPT 1 mM
- 25 mM phosphate buffer + 10 % DMSO
- pH 7.4, T: 37 °C

t = 0 h



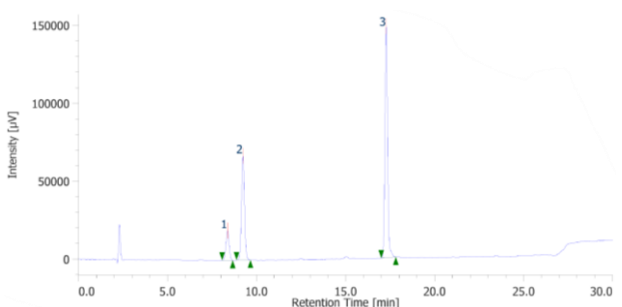
#	Peak Name	CH	tR [min]	Area [µV·sec]	Height [µV]	Area%	Height%	Resolution	Symmetry Factor	Factor
1	Unknown	9	8.34	223487	17741	5.10	5.568	2.674	0.958	1.00000
2	Unknown	9	9.27	4162761	300896	94.9	94.432	N/A	1.022	1.00000
Total				4386248	318637					

t = 1 h



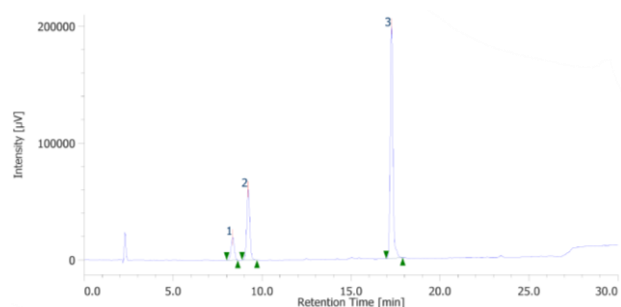
#	Peak Name	CH	tR [min]	Area [µV·sec]	Height [µV]	Area%	Height%	Resolution	Symmetry Factor	Factor
1	Unknown	9	8.33	226422	17859	5.19	4.902	2.485	0.940	1.00000
2	Unknown	9	9.24	1849579	125355	42.4	34.410	24.319	1.058	1.00000
3	Unknown	9	17.3	2285636	221085	52.4	60.688	N/A	1.045	1.00000
Total				4361637	364299					

t = 5 h



#	Peak Name	CH	tR [min]	Area [µV·sec]	Height [µV]	Area%	Height%	Resolution	Symmetry Factor	Factor
1	Unknown	9	8.37	239732	18940	9.26	8.099	2.697	0.973	1.00000
2	Unknown	9	9.24	799346	66791	30.9	28.524	27.986	1.042	1.00000
3	Unknown	9	17.3	1549516	148425	59.9	63.387	N/A	1.063	1.00000
Total				2588594	234156					

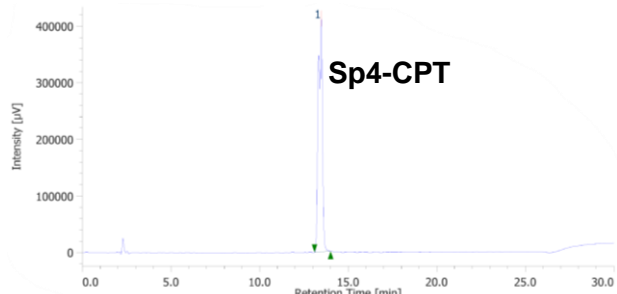
t = 8 h



#	Peak Name	CH	tR [min]	Area [µV·sec]	Height [µV]	Area%	Height%	Resolution	Symmetry Factor	Factor
1	Unknown	9	8.35	248693	19530	8.11	7.016	2.704	0.970	1.00000
2	Unknown	9	9.22	723775	60470	23.6	21.725	28.040	1.040	1.00000
3	Unknown	9	17.3	2094513	198343	68.3	71.259	N/A	1.090	1.00000
Total				3066981	278343					

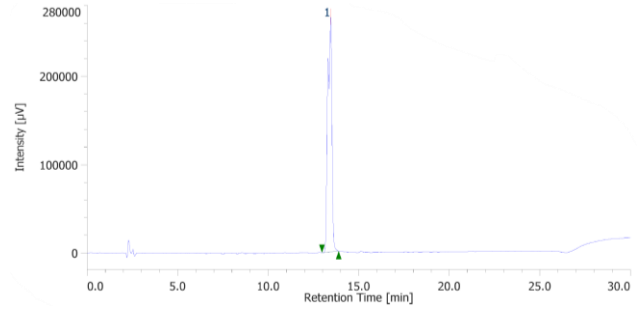
- Sp4-CPT 1 mM
- 25 mM phosphate buffer + 10 % DMSO
- pH 7.4, T: 37 °C

t = 0 h



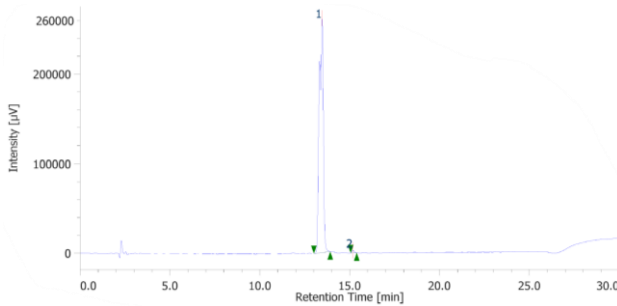
#	Peak Name	CH	tR [min]	Area [µV·sec]	Height [µV]	Area%	Height%	Resolution	Symmetry Factor	Factor
1	Unknown	9	13.5	6716274	411843	100	100.000	N/A	0.802	1.00000
Total				6716274	411843					

t = 1 h



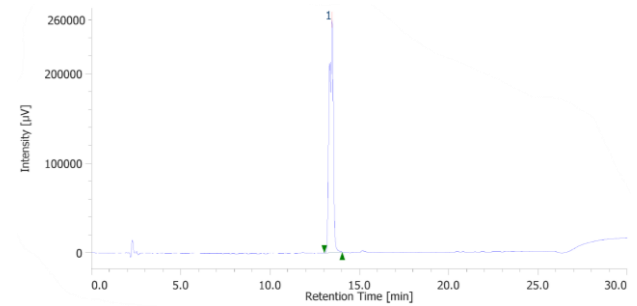
#	Peak Name	CH	tR [min]	Area [µV·sec]	Height [µV]	Area%	Height%	Resolution	Symmetry Factor	Factor
1	Unknown	9	13.4	4242007	265898	100	100.000	N/A	0.801	1.00000
Total				4242007	265898					

t = 5 h



#	Peak Name	CH	tR [min]	Area [µV·sec]	Height [µV]	Area%	Height%	Resolution	Symmetry Factor	Factor
1	Unknown	9	13.5	4125245	261645	99.4	98.935	4.777	0.792	1.00000
2	Unknown	9	15.2	25365	2818	0.611	1.065	N/A	1.288	1.00000
Total				4150610	264463					

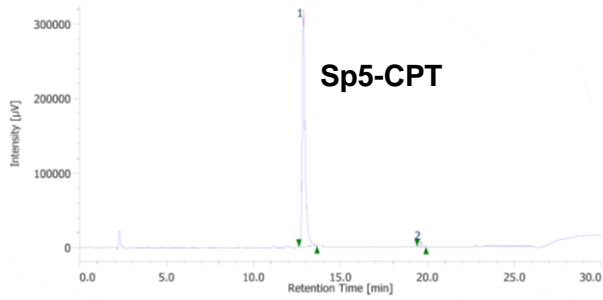
t = 8 h



#	Peak Name	CH	tR [min]	Area [µV·sec]	Height [µV]	Area%	Height%	Resolution	Symmetry Factor	Factor
1	Unknown	9	13.5	4113619	259730	100	100.000	N/A	0.800	1.00000
Total				4113619	259730					

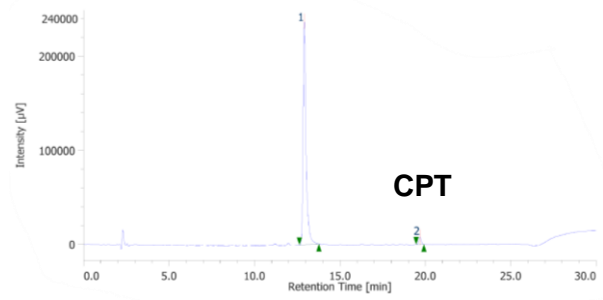
- Sp5-CPT 1 mM
- 25 mM phosphate buffer + 10 % DMSO
- pH 7.4, T: 37 °C

t = 0 h



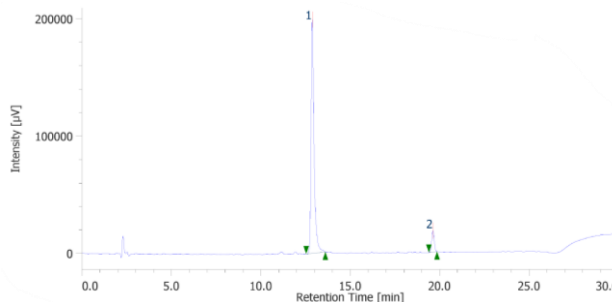
#	Peak Name	CH	tR [min]	Area [µV·sec]	Height [µV]	Area%	Height%	Resolution	Symmetry Factor	Factor
1	Unknown	9	12.9	3646248	307872	98.3	98.042	25.124	1.530	1.00000
2	Unknown	9	19.6	61235	6147	1.65	1.958	N/A	1.147	1.00000
Total				3707483	314019					

t = 1 h



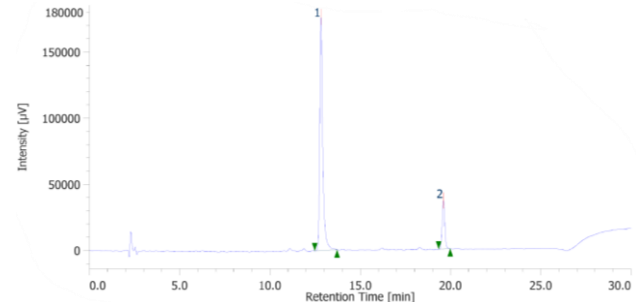
#	Peak Name	CH	tR [min]	Area [µV·sec]	Height [µV]	Area%	Height%	Resolution	Symmetry Factor	Factor
1	Unknown	9	12.9	2835816	237522	97.4	96.923	24.943	1.512	1.00000
2	Unknown	9	19.7	75217	7540	2.58	3.077	N/A	1.005	1.00000
Total				2911033	245062					

t = 5 h



#	Peak Name	CH	tR [min]	Area [µV·sec]	Height [µV]	Area%	Height%	Resolution	Symmetry Factor	Factor
1	Unknown	9	12.9	2309386	199223	92.8	91.633	25.326	1.501	1.00000
2	Unknown	9	19.6	178916	18192	7.19	8.367	N/A	1.014	1.00000
Total				2488302	217415					

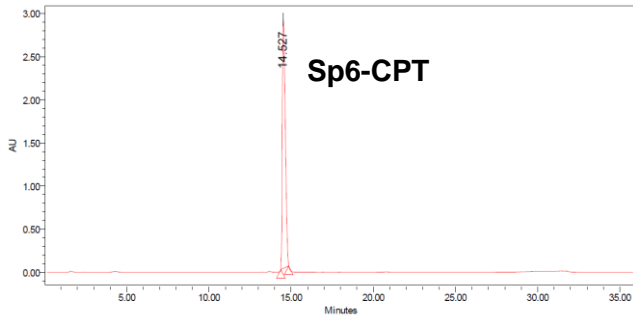
t = 8 h



#	Peak Name	CH	tR [min]	Area [µV·sec]	Height [µV]	Area%	Height%	Resolution	Symmetry Factor	Factor
1	Unknown	9	12.8	2060639	176456	84.5	82.848	25.030	1.484	1.00000
2	Unknown	9	19.6	378397	36532	15.5	17.152	N/A	1.065	1.00000
Total				2439036	212988					

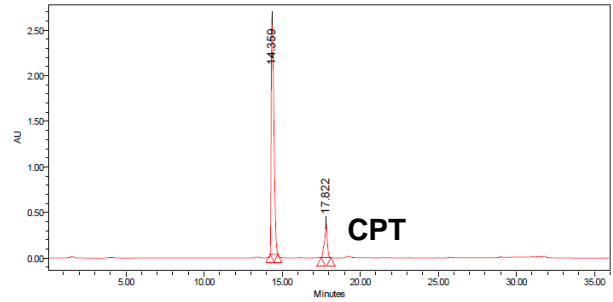
- Sp6-CPT 1 mM
- 25 mM phosphate buffer + 10 % DMSO
- pH 7.4, T: 37 °C

t = 0 h



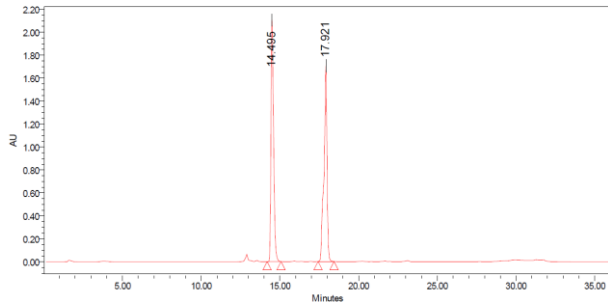
Peak Results						
Name	RT	Area	Height	Amount	Units	% Area
1	14.527	36843380	2907247			100.00

t = 1 h



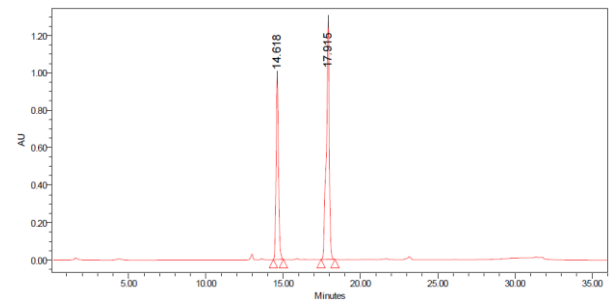
Peak Results						
Name	RT	Area	Height	Amount	Units	% Area
1	14.359	31042815	2612304			86.82
2	17.822	4711406	365275			13.18

t = 5 h



Peak Results						
Name	RT	Area	Height	Amount	Units	% Area
1	14.495	24233861	2124688			51.38
2	17.921	22928771	1702838			48.62

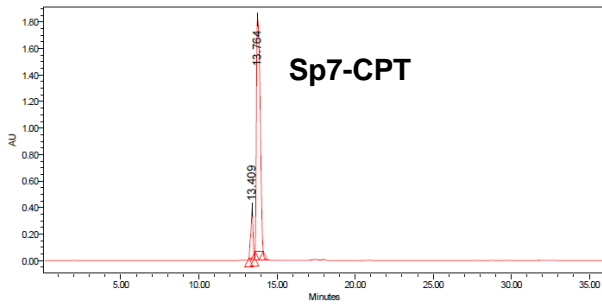
t = 8 h



Peak Results						
Name	RT	Area	Height	Amount	Units	% Area
1	14.618	10477199	973577			38.30
2	17.915	16816806	1276753			61.61

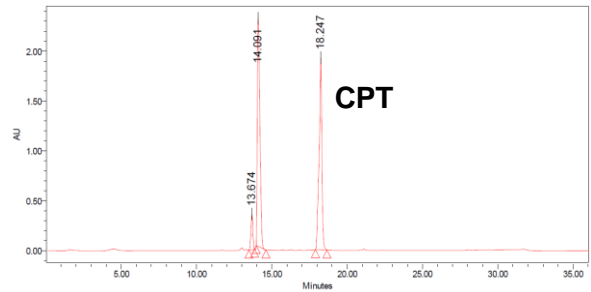
- Sp7-CPT 1 mM
- 25 mM phosphate buffer + 10 % DMSO
- pH 7.4, T: 37 °C

t = 0 h



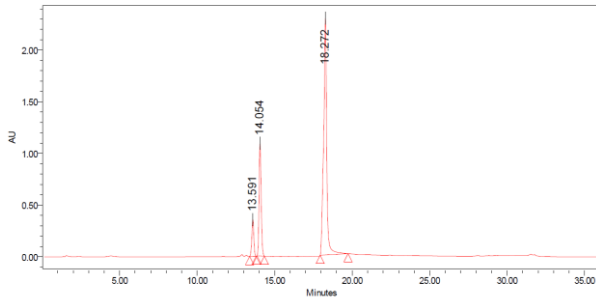
Peak Results						
Name	RT	Area	Height	Amount	Units	% Area
1	13.409	3622851	369571			111.02
2	13.794	29252639	1762899			88.98

t = 1 h



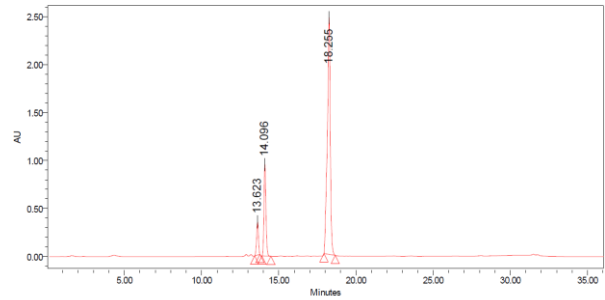
Peak Results						
Name	RT	Area	Height	Amount	Units	% Area
1	13.674	3143655	356143			6.70
2	14.091	27238483	2297449			49.43
3	18.247	24727556	1934621			44.87

t = 5 h



Peak Results						
Name	RT	Area	Height	Amount	Units	% Area
1	13.591	3148905	357395			6.97
2	14.054	10185231	1084594			22.51
3	18.272	31864199	2297143			70.52

t = 8 h

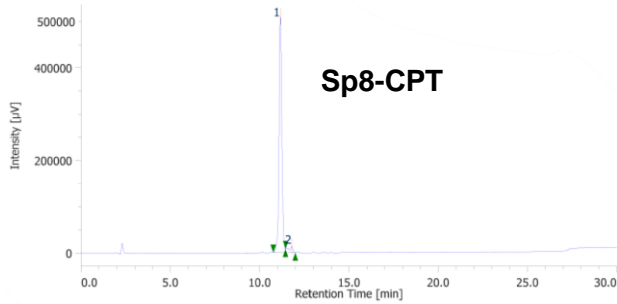


Peak Results						
Name	RT	Area	Height	Amount	Units	% Area
1	13.623	2884549	347109			6.52
2	14.096	8402196	962047			19.13
3	18.265	32666611	2465378			74.35



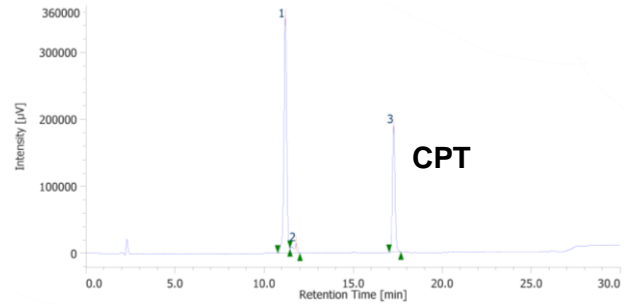
- Sp8-CPT 1 mM
- 25 mM phosphate buffer + 10 % DMSO
- pH 7.4, T: 37 °C

t = 0 h



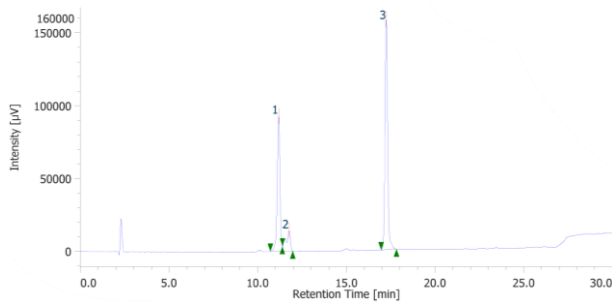
#	Peak Name	CH	tR [min]	Area [µV.sec]	Height [µV]	Area%	Height%	Resolution	Symmetry Factor	Factor
1	Unknown	9	11.2	5536067	509619	95.7	97.418	N/A	0.994	1.00000
2	Unknown	9	11.8	246609	13504	4.26	2.582	N/A	N/A	1.00000
Total				5782676	523123					

t = 1 h



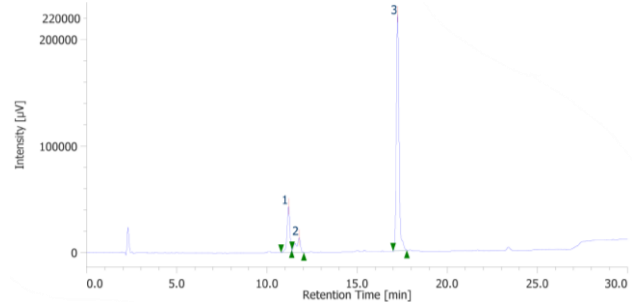
#	Peak Name	CH	tR [min]	Area [µV.sec]	Height [µV]	Area%	Height%	Resolution	Symmetry Factor	Factor
1	Unknown	9	11.2	3755788	351414	63.3	63.417	1.288	0.952	1.00000
2	Unknown	9	11.8	248321	13816	4.19	2.493	11.460	N/A	1.00000
3	Unknown	9	17.3	1925969	188900	32.5	34.089	N/A	1.040	1.00000
Total				5930078	554130					

t = 5 h



#	Peak Name	CH	tR [min]	Area [µV.sec]	Height [µV]	Area%	Height%	Resolution	Symmetry Factor	Factor
1	Unknown	9	11.2	984771	92661	34.2	35.059	1.330	0.896	1.00000
2	Unknown	9	11.8	237584	13794	8.25	5.219	12.346	N/A	1.00000
3	Unknown	9	17.2	1656835	157849	57.5	59.723	N/A	1.066	1.00000
Total				2879190	264304					

t = 8 h

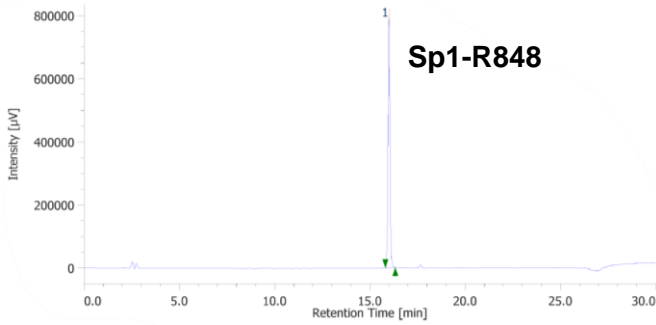


#	Peak Name	CH	tR [min]	Area [µV.sec]	Height [µV]	Area%	Height%	Resolution	Symmetry Factor	Factor
1	Unknown	9	11.2	458103	43196	15.1	15.487	1.337	N/A	1.00000
2	Unknown	9	11.8	243042	13896	7.99	4.982	12.338	N/A	1.00000
3	Unknown	9	17.2	2339308	221827	76.9	79.531	N/A	1.087	1.00000
Total				3040453	278919					

## HPLC Data – Sp-R848 Modules

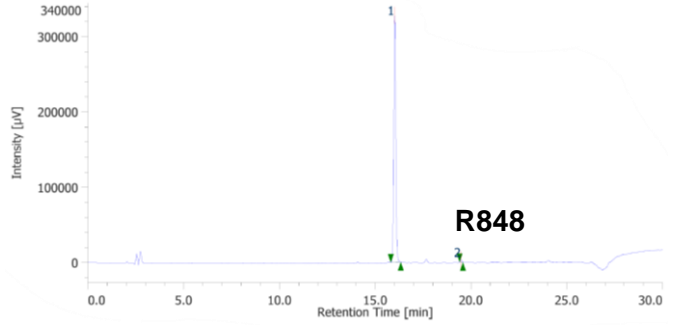
- Sp1-R848 1 mM
- 25 mM phosphate buffer + 10 % DMSO
- pH 7.4, T: 37 °C

t = 0 h



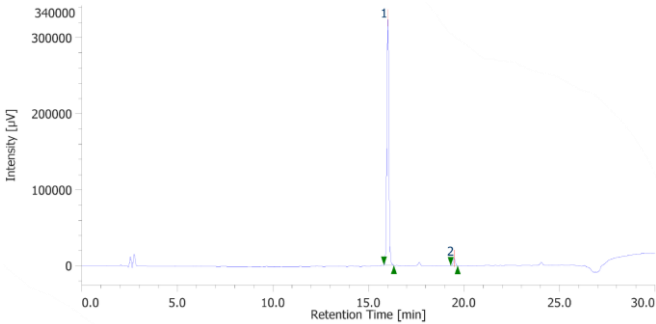
#	Peak Name	CH	tR [min]	Area [µV·sec]	Height [µV]	Area%	Height%	Resolution	Symmetry Factor	Factor
1	Unknown	9	16.0	5678609	793809	100	100.000	N/A	1.092	1.00000
Total				5678609	793809					

t = 2 h



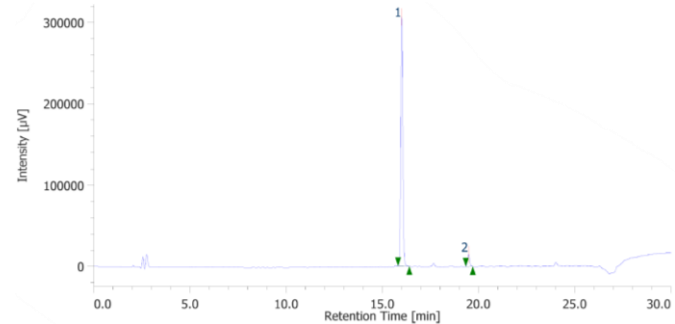
#	Peak Name	CH	tR [min]	Area [µV·sec]	Height [µV]	Area%	Height%	Resolution	Symmetry Factor	Factor
1	Unknown	9	16.0	2425795	327507	99.2	99.053	18.915	1.054	1.00000
2	Unknown	9	19.5	19284	3132	0.789	0.947	N/A	1.018	1.00000
Total				2445079	330639					

t = 5 h



#	Peak Name	CH	tR [min]	Area [µV·sec]	Height [µV]	Area%	Height%	Resolution	Symmetry Factor	Factor
1	Unknown	9	16.0	2419514	325259	97.0	97.153	17.351	1.035	1.00000
2	Unknown	9	19.5	75020	9531	3.01	2.847	N/A	1.021	1.00000
Total				2494534	334790					

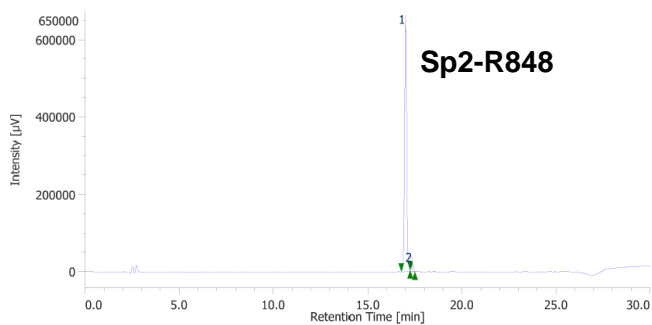
t = 8 h



#	Peak Name	CH	tR [min]	Area [µV·sec]	Height [µV]	Area%	Height%	Resolution	Symmetry Factor	Factor
1	Unknown	9	16.0	2272848	306164	95.2	95.433	17.421	1.038	1.00000
2	Unknown	9	19.5	115411	14653	4.83	4.567	N/A	1.080	1.00000
Total				2388259	320817					

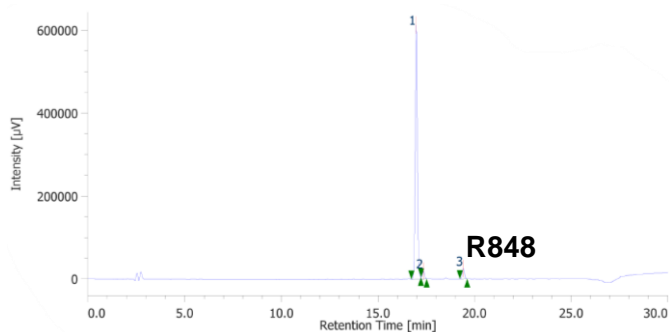
- Sp2-R848 1 mM
- 25 mM phosphate buffer + 10 % DMSO
- pH 7.4, T: 37 °C

t = 0 h



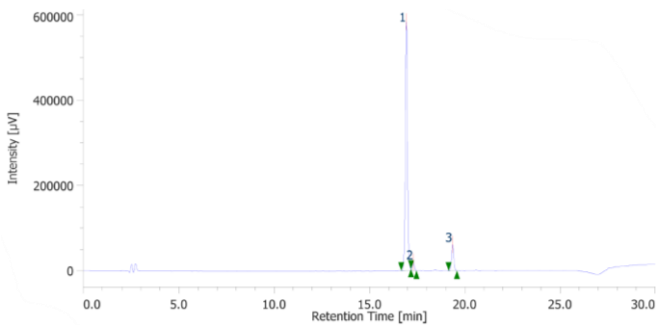
#	Peak Name	CH	tR [min]	Area [µV·sec]	Height [µV]	Area%	Height%	Resolution	Symmetry Factor	Factor
1	Unknown	9	17.0	4942535	639918	97.3	97.265	1.843	1.034	1.00000
2	Unknown	9	17.4	136929	17992	2.70	2.735	N/A	N/A	1.00000
Total				5079464	657910					

t = 2 h



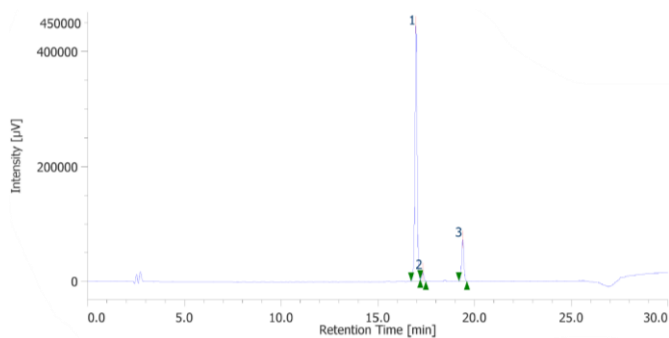
#	Peak Name	CH	tR [min]	Area [µV·sec]	Height [µV]	Area%	Height%	Resolution	Symmetry Factor	Factor
1	Unknown	9	17.0	4712360	612429	93.1	93.355	1.850	1.050	1.00000
2	Unknown	9	17.3	147963	18537	2.92	2.826	9.846	N/A	1.00000
3	Unknown	9	19.4	201432	25057	3.98	3.819	N/A	1.013	1.00000
Total				5061755	656023					

t = 5 h



#	Peak Name	CH	tR [min]	Area [µV·sec]	Height [µV]	Area%	Height%	Resolution	Symmetry Factor	Factor
1	Unknown	9	16.9	4580853	583412	87.6	87.849	1.818	1.008	1.00000
2	Unknown	9	17.3	151319	19358	2.89	2.915	9.907	N/A	1.00000
3	Unknown	9	19.4	499298	61340	9.54	9.236	N/A	1.021	1.00000
Total				5231470	664110					

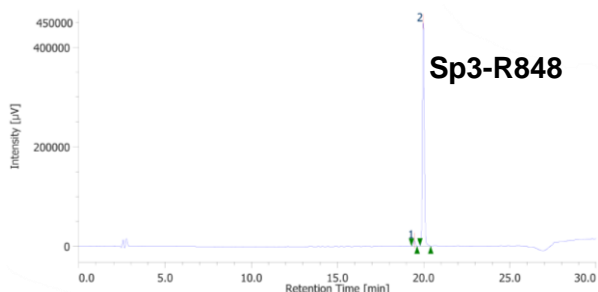
t = 8 h



#	Peak Name	CH	tR [min]	Area [µV·sec]	Height [µV]	Area%	Height%	Resolution	Symmetry Factor	Factor
1	Unknown	9	17.0	3489120	446139	83.1	83.426	1.758	0.968	1.00000
2	Unknown	9	17.3	126154	16079	3.01	3.007	10.086	N/A	1.00000
3	Unknown	9	19.4	581844	72551	13.9	13.567	N/A	1.011	1.00000
Total				4197118	534769					

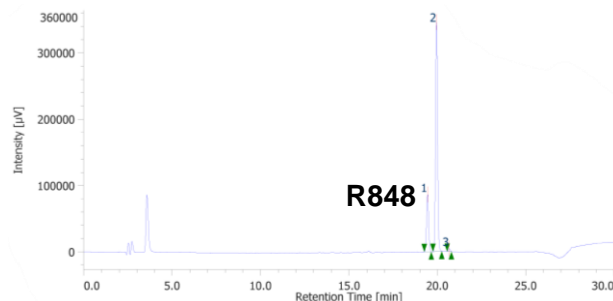
- **Sp3-R848** 1 mM
- 25 mM phosphate buffer + 10 % DMSO
- pH 7.4, T: 37 °C

t = 0 h



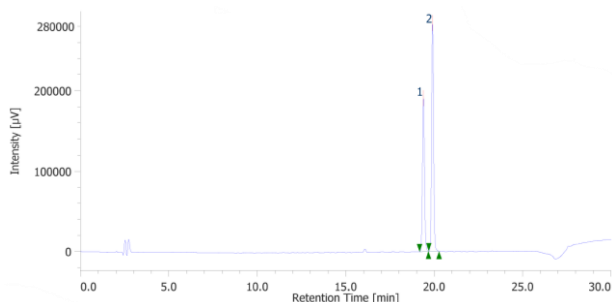
#	Peak Name	CH	tR [min]	Area [µV·sec]	Height [µV]	Area%	Height%	Resolution	Symmetry Factor	Factor
1	Unknown	9	19.5	84535	10698	2.45	2.318	2.567	0.970	1.00000
2	Unknown	9	20.0	3368955	450908	97.6	97.682	N/A	1.097	1.00000
Total				3453490	461606					

t = 2 h



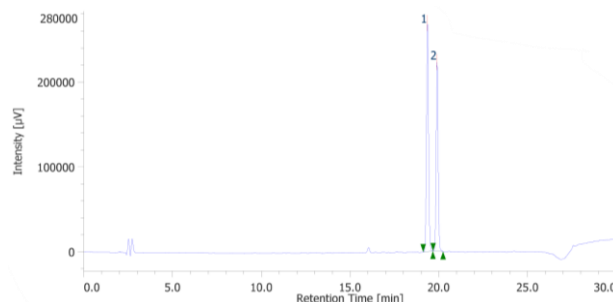
#	Peak Name	CH	tR [min]	Area [µV·sec]	Height [µV]	Area%	Height%	Resolution	Symmetry Factor	Factor
1	Unknown	9	19.4	692868	86311	20.4	19.777	2.483	1.032	1.00000
2	Unknown	9	19.9	2668512	345701	78.7	79.211	3.689	1.075	1.00000
3	Unknown	9	20.7	30567	4420	0.901	1.013	N/A	1.006	1.00000
Total				3391947	436432					

t = 5 h



#	Peak Name	CH	tR [min]	Area [µV·sec]	Height [µV]	Area%	Height%	Resolution	Symmetry Factor	Factor
1	Unknown	9	19.4	1522958	190504	41.1	40.208	2.558	1.059	1.00000
2	Unknown	9	19.9	2179195	283292	58.9	59.792	N/A	1.062	1.00000
Total				3702153	473796					

t = 8 h

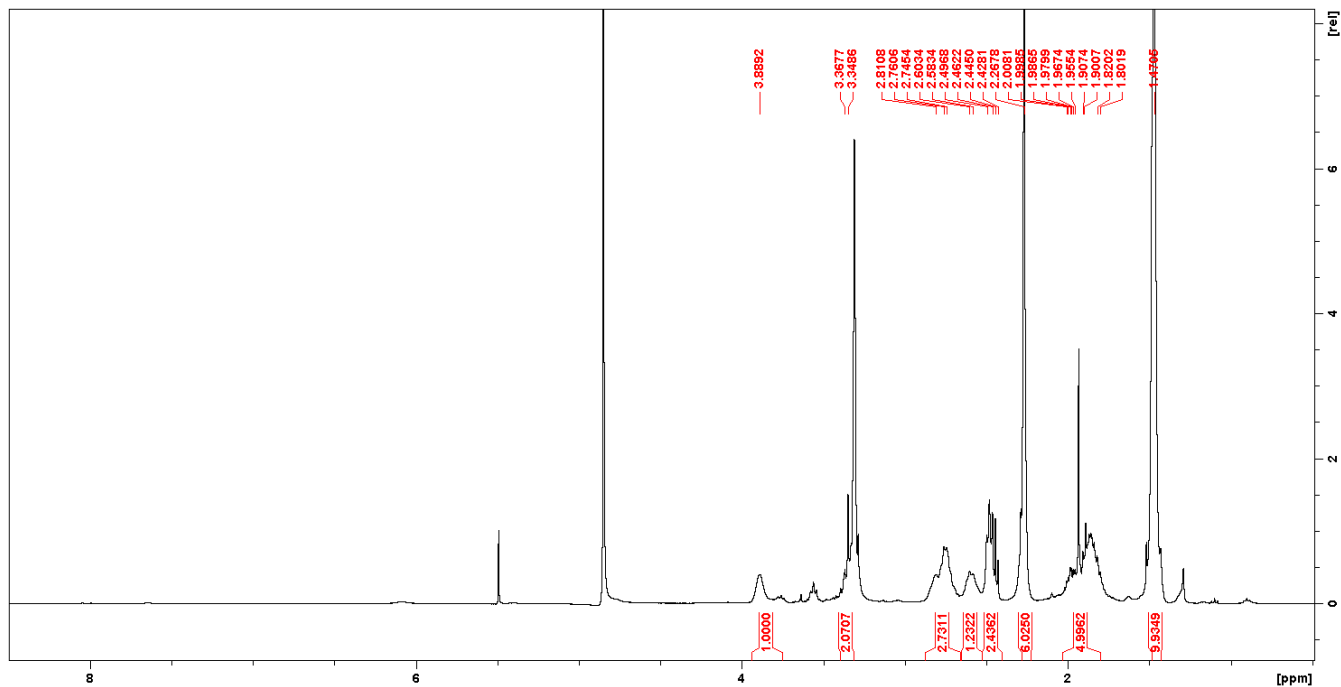


#	Peak Name	CH	tR [min]	Area [µV·sec]	Height [µV]	Area%	Height%	Resolution	Symmetry Factor	Factor
1	Unknown	9	19.4	2165730	268721	56.1	54.701	2.670	1.052	1.00000
2	Unknown	9	19.9	1697404	222531	43.9	45.299	N/A	1.061	1.00000
Total				3863134	491252					

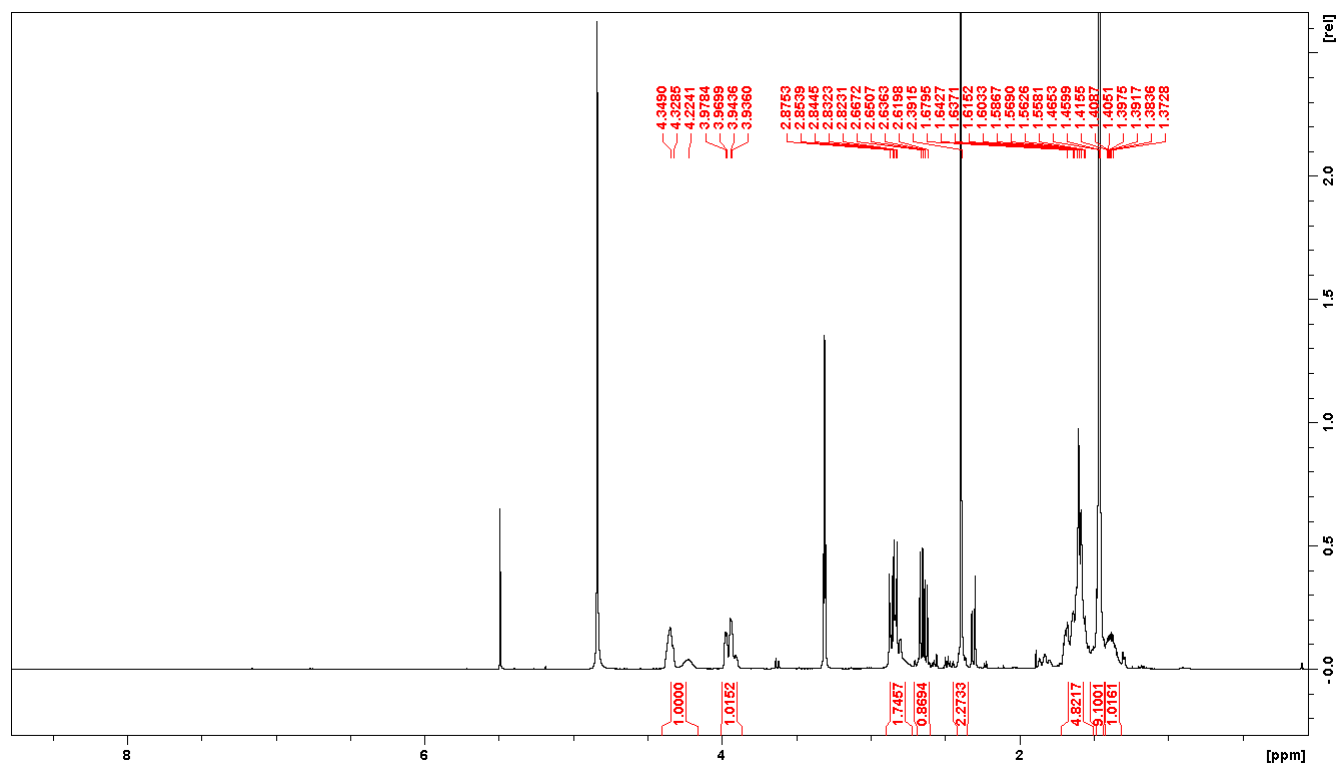
## NMR Spectra

*Tert-butyl (S)-2-(((2-(dimethylamino)ethyl)amino)methyl)pyrrolidine-1-carboxylate*

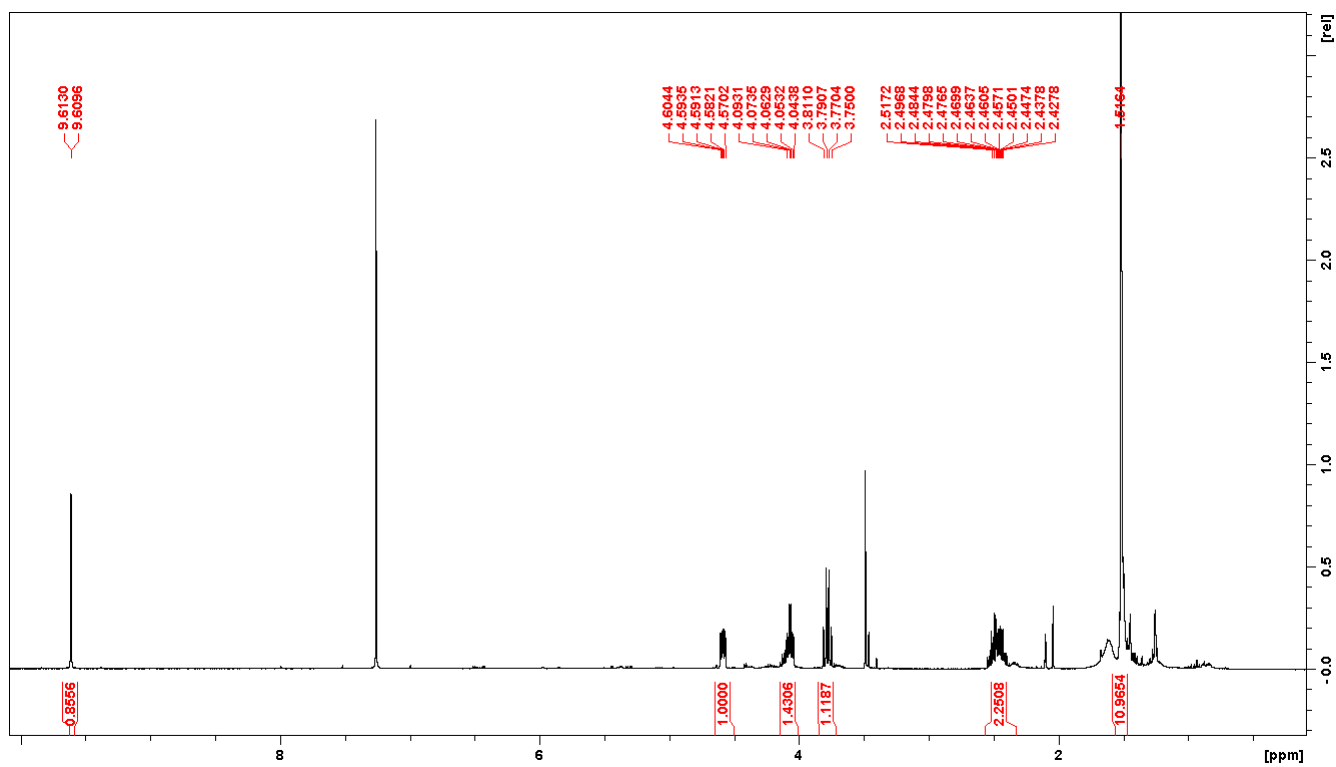
(3)



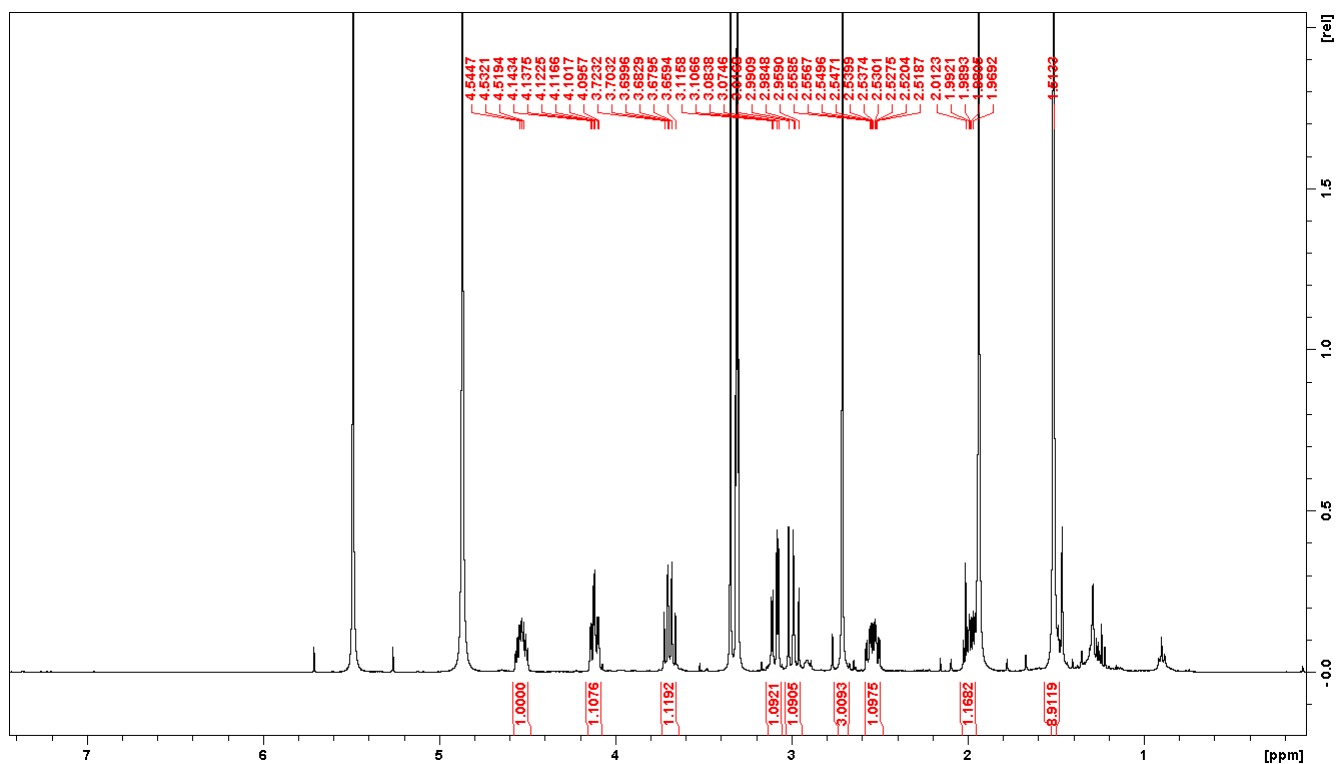
*Tert-butyl 2-((methylamino)methyl)piperidine-1-carboxylate (5)*



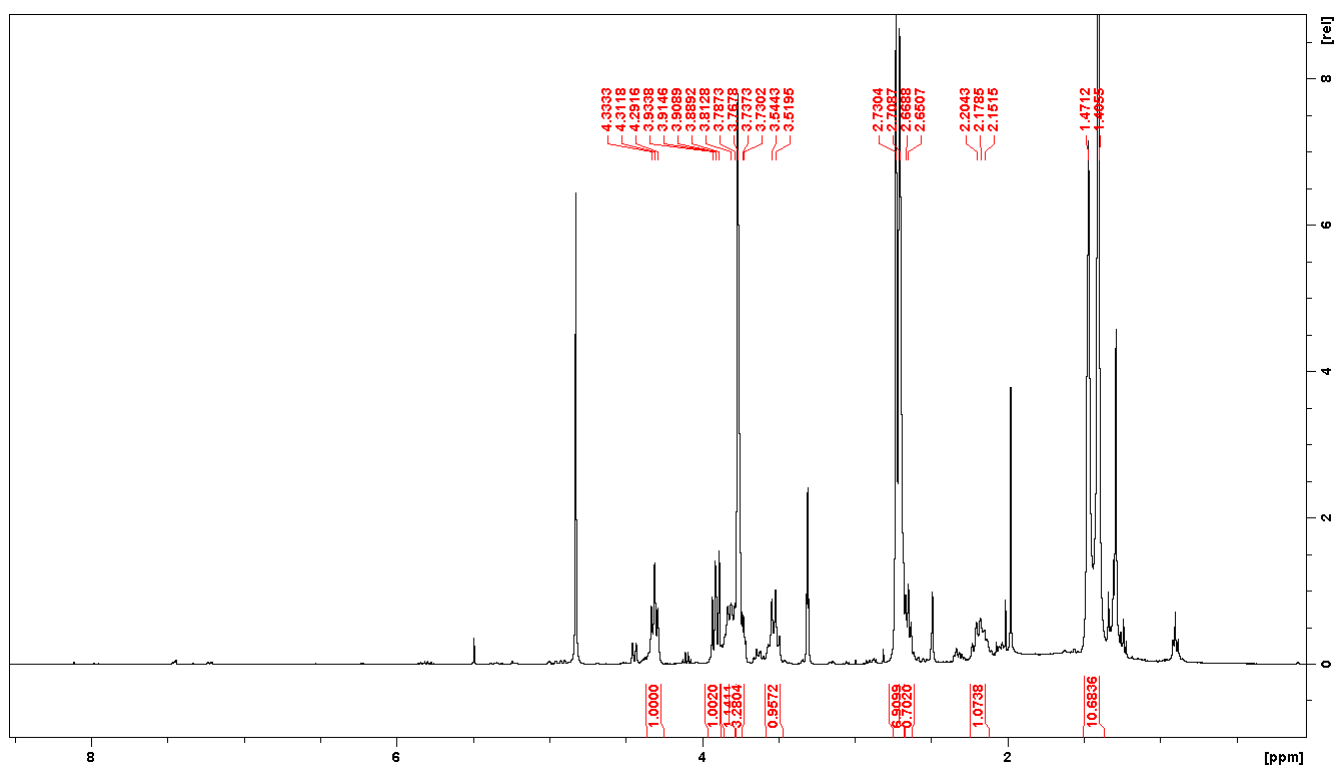
*Tert-butyl (S)-3-formylisoxazolidine-2-carboxylate (7)*



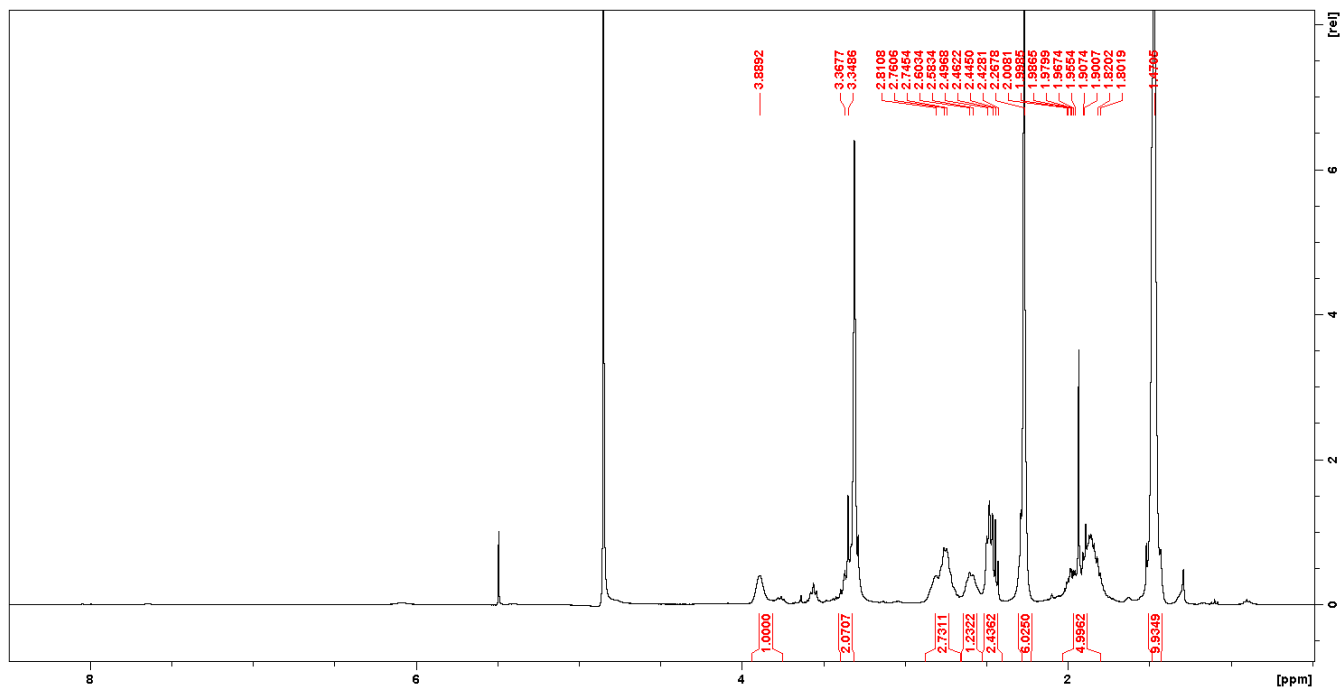
*O-acetyl-N-(((S)-2-(tert-butoxycarbonyl)isoxazolidin-3-yl)methyl)-N-methylhydroxylammonium (8)*



1-(tert-butyl) 2-methyl (2S,4S)-4-(dimethylamino)pyrrolidine-1,2-dicarboxylate (**10**):

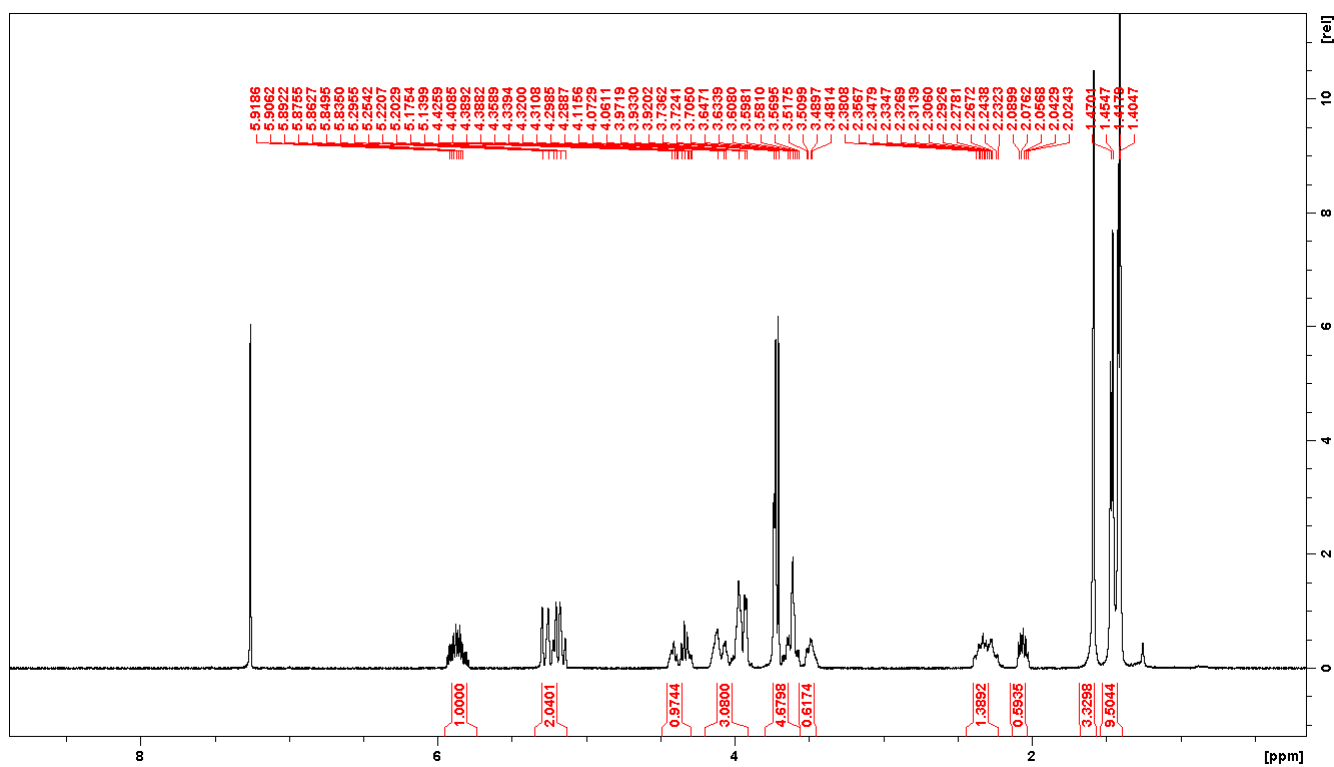


Tert-butyl 2-(((3-(dimethylamino)propyl)amino)methyl)pyrrolidine-1-carboxylate (**13**)

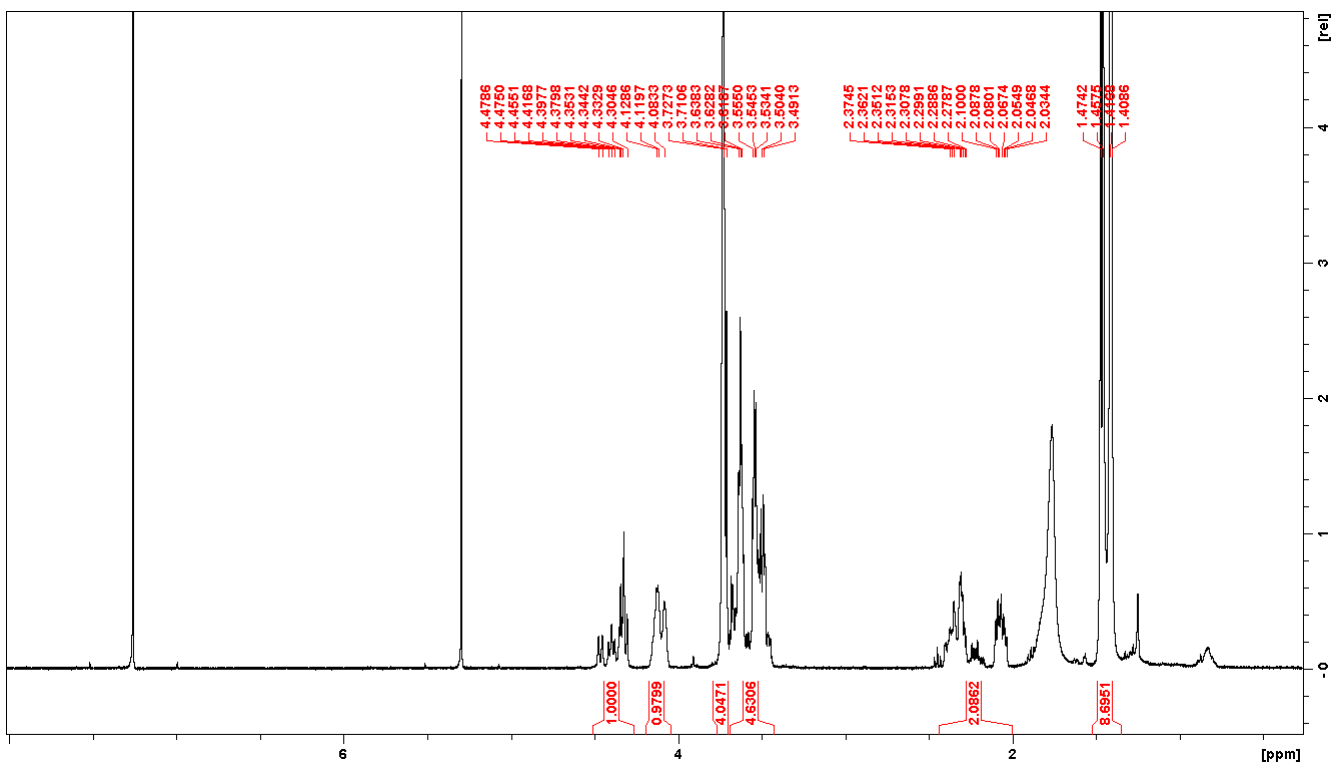




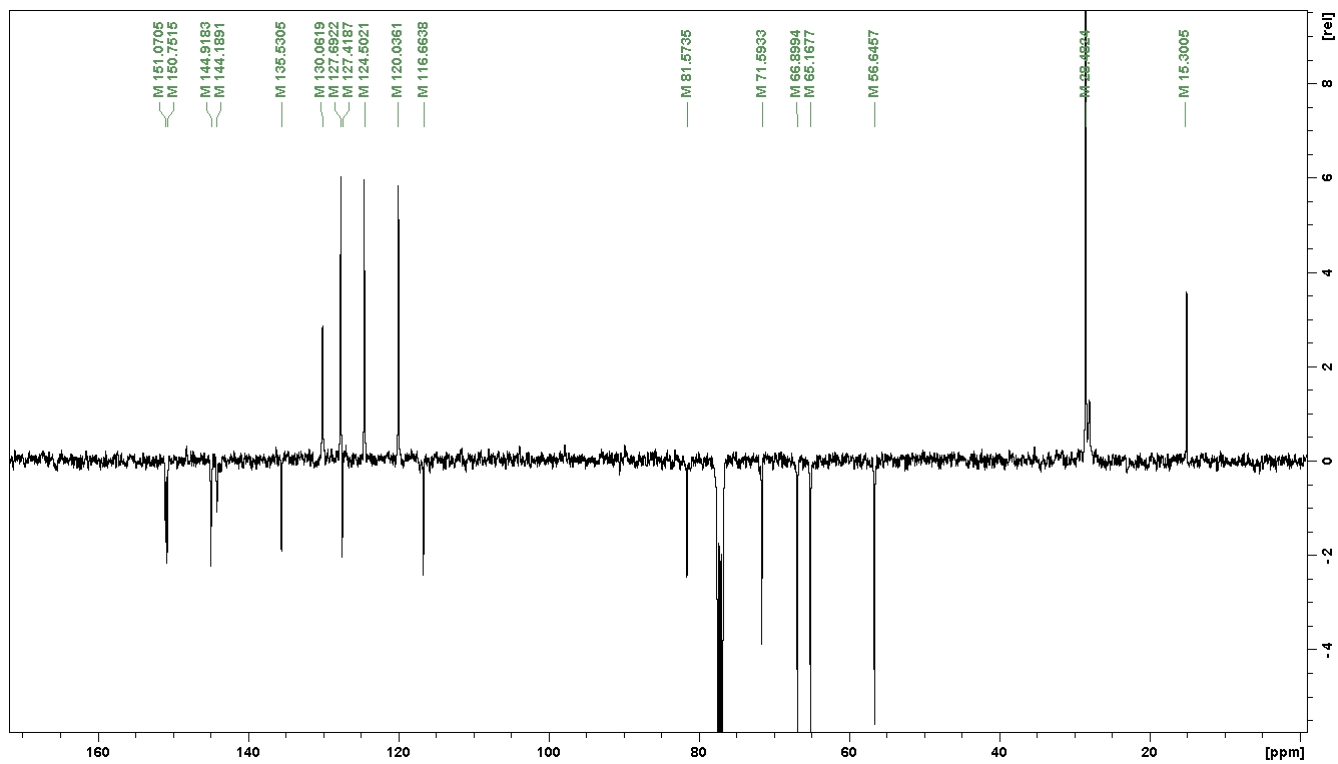
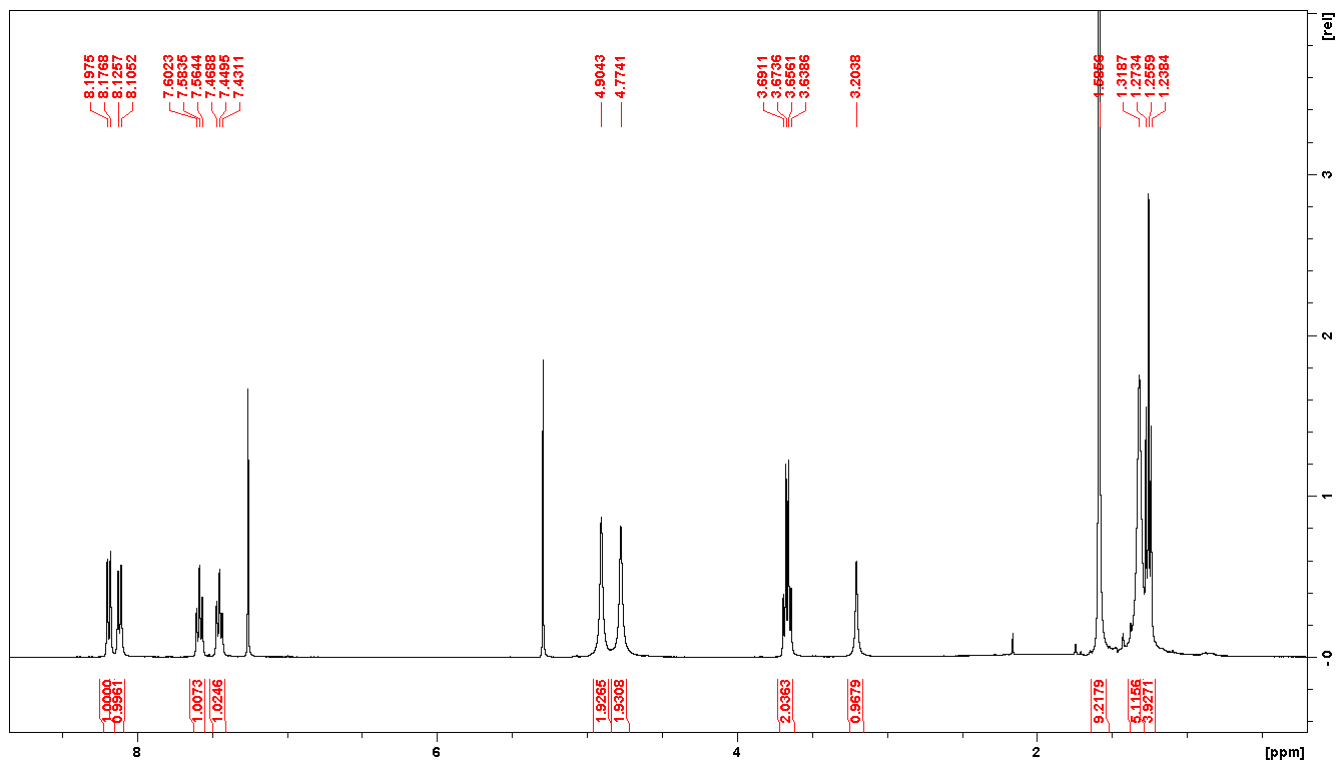
*Boc-Hyp(All)-OMe (15)*



*Boc-Hyp(2-hydroxyethoxy)-OMe (17)*



# Boc-R848



# R848-PNP

